DOI: 10.1093/jnci/djq343
Advance Access publication on September 17, 2010.

ARTICLE

CSPG4 Protein as a New Target for the Antibody-Based Immunotherapy of Triple-Negative Breast Cancer

Xinhui Wang,Takuya Osada, Yangyang Wang, Ling Yu, Koichi Sakakura, Akihiro Katayama, James B. McCarthy, Adam Brufsky, Mamatha Chivukula, Thaer Khoury, David S. Hsu, William T. Barry, H. Kim Lyerly, Timothy M. Clay, Soldano Ferrone

Manuscript received September 30, 2009; revised August 9, 2010; accepted August 10, 2010.

Correspondence to: Soldano Ferrone, MD, PhD, University of Pittsburgh Cancer Institute, 5117 Centre Ave, Pittsburgh, PA 15213 (e-mail: ferrones@upmc.edu).

Background The cell surface proteoglycan, chondroitin sulfate proteoglycan 4 (CSPG4), is a potential target for monoclonal antibody (mAb)–based immunotherapy for many types of cancer. The lack of effective therapy for triple-negative breast cancer (TNBC) prompted us to examine whether CSPG4 is expressed in TNBC and can be targeted with CSPG4-specific mAb.

Methods CSPG4 protein expression was assessed in 44 primary TNBC lesions, in TNBC cell lines HS578T, MDA-MB-231, MDA-MB-435, and SUM149, and in tumor cells in pleural effusions from 12 metastatic breast cancer patients. The effect of CSPG4-specific mAb 225.28 on growth, adhesion, and migration of TNBC cells was tested in vitro. The ability of mAb 225.28 to induce regression of tumor metastases (n = 7 mice) and to inhibit spontaneous metastasis and tumor recurrence (n = 12 mice per group) was tested in breast cancer models in mice. The mechanisms responsible for the antitumor effect of mAb 225.28 were also investigated in the cell lines and in the mouse models. All statistical tests were two-sided.

Results CSPG4 protein was preferentially expressed in 32 of the 44 (72.7%) primary TNBC lesions tested, in TNBC cell lines, and in tumor cells in pleural effusions from 12 metastatic breast cancer patients. CSPG4-specific mAb 225.28 statistically significantly inhibited growth, adhesion, and migration of TNBC cells in vitro. mAb 225.28 induced 73.1% regression of tumor metastasis in a TNBC cell–derived experimental lung metastasis model (mAb 225.28 vs control, mean area of metastatic nodules = 44590.8 vs 165950.8 μm^2; difference of mean = 121360.0 μm^2, 95% confidence interval = 91010.7 to 151709.4 μm^2; $P < .001$). Additionally, mAb 225.28 statistically significantly reduced spontaneous lung metastases and tumor recurrences in an orthotopic xenograft mouse model. The mechanisms responsible for antitumor effect included increased apoptosis and reduced mitotic activity in tumor cells, decreased blood vessel density in the tumor microenvironment, and reduced activation of signaling pathways involved in cell survival, proliferation and metastasis.

Conclusions This study identified CSPG4 as a new target for TNBC. The antitumor activity of CSPG4-specific mAb was mediated by multiple mechanisms, including the inhibition of signaling pathways crucial for TNBC cell survival, proliferation, and metastasis.

J Natl Cancer Inst 2010;102:1496–1512

Based on gene expression profiling using the DNA microarray technology, breast tumors are classified into distinct molecular subtypes that are associated with different clinical outcomes (1–3). The main subtypes are normal breast-like, HER2 (also known as v-erb-b2 erythroblastic leukemia viral oncogene homolog 2, neuro/glioblastoma derived oncogene homolog) overexpressing, luminal A and B, and basal-like breast cancer. The normal breast-like cancer cells display high expression of genes characteristic of basal epithelial cells and adipose cells and low expression of genes characteristic of luminal epithelial cells (4). The HER2-positive ($HER2^+$) cancer cells show overexpression of HER2 receptors and several other genes of the *HER2* amplicon (3). The luminal tumors express high levels of luminal cytokeratins and genetic markers of the luminal epithelial cells (5). They are subdivided into luminal A subtype that are predominantly estrogen receptor–positive (ER^+) and are histologically low-grade tumors, and luminal B subtype that are also mostly ER^+ but can express low levels of ER and are often histologically high-grade tumors (5). The basal-like breast cancers do not express several genes that typify myoepithelial cells of normal breast tissue such as luminal cytokeratins, smooth muscle–specific markers, and certain integrins (2). However, some basal-like cancers express high levels of cytokeratins such as cytokeratin 5, growth factor receptors such as epidermal growth factor receptor and tyrosine kinase receptor c–KIT (also known as v-kit

Hardy-Zuckerman 4 feline sarcoma viral oncogene homolog), and growth factors such as hepatocyte growth factor and insulinlike growth factor (2,3).

Because gene expression profiling is not widely available clinically, most oncologists rely on other methods such as immunohistochemistry (IHC) to characterize clinical specimens. Unfortunately, IHC testing for basal-like breast cancer (6) has not gained wide acceptance because of the difficulty in combining the multiple IHC markers needed to characterize the basal-like phenotype and the incomplete concordance of these IHC markers with the molecular classification defined by gene expression pattern. Therefore, in the clinical setting, the triple-negative breast cancer (TNBC), characterized by ER^-/progesterone receptor–negative (PR^-)/$HER2^-$ phenotype, is generally accepted as a proxy for the basal-like subtype. The TNBC phenotype has a particularly unfavorable clinical prognosis, despite increased sensitivity to standard cytotoxic chemotherapy regimens (7). An emerging concept is that tumor recurrences and unfavorable clinical prognosis of TNBC are because of the presence of a population of chemotherapy- and radiotherapy-resistant cancer stem cells (CSCs) within tumors (8). The human breast CSCs are characterized by high expression of CD44 protein and low expression of CD24 protein ($CD44^{hi}$/$CD24^{lo/-}$) and have the functional characteristics of CSCs (9). These findings suggest that one potential basis for the aggressive nature of both basal-like breast cancer and TNBC, and their resistance to chemo- and radiotherapy, is the presence of a substantial CSC subpopulation. A few recent studies have provided evidence for a high frequency of CSC, characterized by the $CD44^{hi}$/$CD24^{lo/-}$ phenotype, in basal-like breast cancer (10–12). Similarly, TNBC is also reportedly enriched in the $CD44^{hi}$/$CD24^{lo/-}$ phenotype (13). Because of the lack of expression of HER2 and hormone receptors ER and PR, TNBC does not benefit from the tailored therapies that are available to target ER or HER2 expression and/or function (7). Furthermore, targeting the epidermal growth factor receptor that is overexpressed in metastatic TNBC with cetuximab has shown disappointing results in clinical trials (14). These findings emphasize the need to develop effective therapeutic strategies for this type of breast cancer.

In this study, we investigated whether chondroitin sulfate proteoglycan 4 (CSPG4), a tumor antigen (15), is expressed by TNBC cells and whether CSPG4 protein might serve as a clinical target. CSPG4, also known as high–molecular weight melanoma–associated antigen or melanoma chondroitin sulfate proteoglycan, is a membrane-bound proteoglycan that consists of an *N*-linked 280 kDa glycoprotein and a 450 kDa chondroitin sulfate proteoglycan (15). It was originally identified on the surface of melanoma cells with monoclonal antibodies (mAbs) (16); more recently, it has been found to be expressed on the surface of differentiated malignant cells, progenitor cells, and CSCs in various types of tumors (17). CSPG4, a phylogenetically conserved protein (15), has been shown to play an important role in growth, migration, and metastatic dissemination of tumor cells (17). Whether the ability of CSCs to migrate and metastasize (9) is attributed to the expression and functional properties of CSPG4 remains to be determined.

CSPG4 was used as a target for immunotherapy of melanoma because of its high expression in at least 80% of melanoma lesions with limited inter- and intra-lesional heterogeneity and its restricted distribution in normal tissues (15). Its clinical relevance is indicated by the statistically significant increase in survival of melanoma patients who developed CSPG4-specific antibodies following active-specific immunotherapy (18). The molecular mechanisms underlying this finding have not been characterized. Therefore, we aimed to investigate whether CSPG4-specific mAbs can inhibit tumor recurrence and metastases using human tumor xenografts of TNBC cells in immunodeficient mice. Our objectives included investigation of the underlying mechanisms of inhibition by studying the effect of CSPG4-specific mAb on growth, adhesion, and migration of TNBC cells, as well as activation of signaling pathways important for tumor cell growth, migration, and survival.

CONTEXT AND CAVEATS

Prior knowledge

CSPG4 protein expressed in 80% of melanoma lesions, and many other human malignancies has shown clinical benefits as an immunotherapy target in melanoma patients. Triple-negative breast tumors are resistant to chemo- and radiotherapy, so it is important to identify new therapeutic targets.

Study design

CSPG4 expression was tested in triple-negative breast cancer (TNBC) cell lines and patient tumors. The immunotherapeutic efficacy of CSPG4-specific monoclonal antibody against tumor growth, metastasis, and recurrence was tested in TNBC xenograft mouse models.

Contribution

CSPG4 was preferentially expressed in TNBC cells. Mice treated with CSPG4-specific monoclonal antibody showed inhibition of tumor growth, metastasis, and recurrence.

Implications

CSPG4 protein is a therapeutic target in breast tumors with TNBC phenotype.

Limitations

The study included only a small number of patients. The antitumor activity of CSPG4-specific monoclonal antibody was also not tested in patient tumor-derived TNBC xenografts in mice. Results of this preclinical study may not be predictive of clinical success.

From the Editors

Patients, Materials, and Methods

Cell Culture and Reagents

The TNBC cell lines HS578T, MDA-MB-231, MDA-MB-435, and SUM149, and the luminal breast cancer cell lines MCF7, SK-BR-3, and T47D (19) were obtained from the Duke Comprehensive Cancer Center Cell Culture Facility. The cell lines were analyzed for the expression of HER2, ER, and PR by flow cytometry analysis (data not shown) to confirm the phenotypes (20,21). The TNBC phenotype ($HER2^-$/ER^-/PR^-) was confirmed in HS578T, MDA-MB-231, MDA-MB-435, and SUM149 cell lines; the luminal phenotype ($HER2^{lo}$/ER^+/PR^+) was confirmed in MCF7 and T47D cell lines; and the luminal phenotype ($HER2^{hi}$/ER^-/PR^-) was confirmed in SK-BR-3 cell line (data not shown).

The human melanoma cell line M14 (22), one of the few melanoma cell lines with no detectable CSPG4 protein expression, was used as the negative control, and the M14 cell line stably transfected with CSPG4 in our laboratory was used as the CSPG4-expressing cell line, M14/CSPG4 (22). Cells were maintained in RPMI 1640 medium (Mediatech, Inc, Herndon, VA) supplemented with 10% fetal calf serum (Atlanta Biologicals, Lawrenceville, GA), penicillin (100 U/mL; Invitrogen, Carlsbad, CA), streptomycin (100 μg/mL; Invitrogen), and glutamine (2.92 mg/mL; Invitrogen) at 37°C in a humidified 5% CO_2 incubator. The M14/CSPG4 cells were grown in RPMI 1640 medium supplemented with geneticin (G418) (400 μg/mL; Invitrogen). The phenotype of M14 and M14/CSPG4 cell lines was verified by assessing the expression of CSPG4 protein by flow cytometry analysis.

Pleural Effusions and Isolation of Tumor Cells From Patients

Pleural effusions, which were used as a source of breast tumor cells, were drained from 14 metastatic breast cancer patients using a PleurX catheter kit (Denver Biomedical, Golden, CO) to collect the fluid. Approximately 500 mL–2 L of pleural effusion fluid was processed from all 14 patients to collect the breast tumor cells. The tumor cells were separated by a Ficoll (Invitrogen) density gradient centrifugation at 1800*g* for 20 minutes at room temperature using Sorvall RT 6000D Refrigerated Centrifuge (Sorvall, Buckinghamshire, UK) to remove tissue debris and red blood cells. Isolated tumor cells were cryopreserved in 90% fetal calf serum and 10% dimethyl sulfoxide (Invitrogen). Typical yields of tumor cells were 2.0×10^8 to 3.0×10^{11} cells per liter of pleural fluid based on flow cytometry and trypan blue dye exclusion method of cell counting. Breast carcinoma cells were identified by gating out hematopoietic cells from the flow cytometry analysis. When a sufficient number of cells was available, they were stained for HER2 and carcinoembryonic antigen expression. A cell and tissue procurement protocol approved by the Duke University's Institutional Review Board was used. All patient samples were de-identified so patient demographic data were not available.

Monoclonal and Polyclonal Antibodies

All the mouse hybridomas used to produce mAbs in our laboratory were developed by us (16,23–27), with the exception of hybridoma HC-10 (28) that was developed by Dr H. Ploegh (Whitehead Institute, Boston, MA) and kindly provided to us. The mAbs 225.28, 763.74, TP41.2, and TP61.5 recognize distinct and spatially distant epitopes of CSPG4 and do not cross-inhibit each other's binding to CSPG4-positive cells (15,16,25,26). The mAb D2.8.5-C4B8 recognizes an epitope of CSPG4 in formalin-fixed paraffin-embedded (FFPE) tissue sections; this epitope is spatially distant from the epitopes recognized by the other four CSPG4-specific mAbs. The anti-idiotypic mAb F3-C25 (23) and the anti-idiotypic mAb MK2-23 (24) recognize an idiotope in the antigen-combining site of the HLA class II antigen–specific mAb CR11-462 and of the CSPG4-specific mAb 763.74, respectively; both were used as isotype controls. The HLA class I heavy chain–specific mAb HC-10 (28) and the calnexin-specific mAb TO-5 (27) were used to detect HLA class I heavy chain and calnexin, respectively; both were used as loading controls in immunoblot assays. All mAbs are IgG1, except mAbs 225.28, F3-C25, and HC-10, which are IgG2a isotypes. The mAbs were purified from mouse ascitic fluid by sequential ammonium sulfate and caprylic acid precipitation (29).

Ready-to-use mouse anti-human ER mAb (clone 6F11) and mouse anti-human PR mAb (clone 1A6) were purchased from Ventana Medical Systems, Inc (Tucson, AZ). Rabbit anti-mouse IgG–phycoerythrin (PE) antibodies were purchased from Dako North America, Inc (Carpinteria, CA). The following mAbs were purchased from BD Pharmingen (San Jose, CA)—mouse anti-human CD24-fluorescein isothiocyanate (FITC), mouse anti-human CD44-allophycocyanin, mouse anti-human CD45-peridinin chlorophyll protein, mouse anti-human HER2-PE, mouse anti-human CD2-PE, mouse anti-human CD3-PE, mouse anti-human CD10-PE, mouse anti-human CD16-PE, mouse anti-human CD18-PE, mouse anti-human CD31-PE, mouse anti-human CD140b-PE, and unconjugated rat anti-mouse CD31 (also known as platelet/endothelial cell adhesion molecule, PECAM1). Mouse anti-human CD64-PE mAb was purchased from R&D Systems (Minneapolis, MN); rabbit anti-human ER-FITC mAb and rabbit IgG-FITC were purchased from Abcam (Cambridge, MA); and mouse anti-human carcinoembryonic antigen-PE mAb was purchased from Sanquin (Amsterdam, the Netherlands).

Mouse anti-human focal adhesion kinase (FAK, also known as protein tyrosine kinase 2) mAb and mouse anti-phosphorylated human FAK (Tyr397) mAb were purchased from BD Transduction Laboratories (San Jose, CA). Mouse anti-human ERK1/2 (extracellular signal-regulated kinases 1 and 2; also known as mitogen-activated protein kinase 1 and 3) mAb and rabbit anti-phosphorylated human ERK1/2 (Thr202/Tyr204) mAb; rabbit anti-human AKT (v-akt murine thymoma viral oncogene homolog 1, Akt1) mAb and rabbit anti-phosphorylated human AKT (Ser473) mAb; and rabbit anti-phosphorylated human Histone H3 (Ser10) antibodies were purchased from Cell Signaling Technology (Beverly, MA). Mouse anti-human protein kinase C, alpha (PKCα, also known as PRKCA) mAb was purchased from Sigma-Aldrich, Inc (St Louis, MO). Goat anti-mouse IgG–peroxidase antibodies and goat anti-rabbit IgG–peroxidase antibodies were purchased from Jackson ImmunoResearch Laboratories, Inc (West Grove, PA).

Gene Expression Analysis

The microarray mRNA expression data were obtained from a publicly available, clinically annotated, breast cancer dataset [National Center for Biotechnology Information Gene Expression Omnibus, accession number GSE5460 (30), consisting of 125 treatment-naive breast tumor samples obtained at the time of surgery and subgrouped according to hormone receptor status (ER^-/$HER2^-$, ER^-/$HER2^+$, ER^+/$HER2^-$, and ER^+/$HER2^+$] (31). For each subgroup, the corresponding mRNA expression levels of CSPG4 were obtained (microarray product information: HG-U133 Plus 2.0 [Affymetrix, Santa Clara, CA]; probe set: 204736_s_at and 214297_at). The differences in expression among the subgroups were evaluated using the nonparametric Kruskal–Wallis test, and pairwise comparisons of ER^-/$HER2^-$ to other subgroups were reported as Mann–Whitney *U* tests using a Bonferroni threshold for multiple comparisons. For all statistical analyses, GraphPad Prism Software, version 4.03 (GraphPad Software, La Jolla, CA),

was used. All two-sided *P* values less than .05 were considered statistically significant.

IHC Staining of Patient-Derived Breast Tumors

Four-micrometer thick sections of FFPE breast tumors surgically removed from patients were stained with ER-specific mAb (clone 6F11, 1:25 dilution) and PR-specific mAb (clone 1A6, 1:20 dilution), respectively, according to the manufacturer's instructions, using the BenchMark XT (Ventana Medical Systems, Inc). HER2 protein expression was assessed using the Food and Drug Administration–approved Hercept-Test (Dako North America, Inc) according to the manufacturer's instructions. ER and PR expression was scored on the basis of nuclear staining, whereas HER2 protein expression was scored on the basis of cytoplasmic membrane staining. ER and PR expression was scored positive when nuclear staining was detected in at least 1% of tumor cells, and HER2 expression was scored positive when cytoplasmic membrane staining was detected in at least 1% of tumor cells. The phenotype of the tumors was provided by the Department of Pathology, Magee Women's Hospital (Pittsburgh, PA). The staining was done once. Twenty-eight tumors of ER^+ and 18 tumors of $HER2^+$ invasive breast carcinomas, and 44 tumors of TNBC ($ER^-/PR^-/HER2^-$) were used for the study. All tumors were reviewed by a pathologist, and invasive carcinoma was confirmed.

IHC Staining of CSPG4 Protein

Tissue sections were deparaffinized with 100% xylene for 20 minutes at room temperature and rehydrated with decreasing concentrations (100%, 90%, 80%, and 70%) (vol/vol) of ethyl alcohol. Antigen retrieval was performed by boiling the sections in 1 mM EDTA (pH 8.0) for 15 minutes. Slides were treated with 3% hydrogen peroxide, 1% bovine serum albumin (BSA) (Invitrogen), and 5% normal horse serum in Tris-buffered saline (25 mM Tris [pH 7.4], 150 mM NaCl) containing 0.1% Tween 20 (Sigma-Aldrich, Inc) and incubated in a closed humid chamber overnight at 4°C with the CSPG4-specific mAb D2.8.5-C4B8 (3 μg/mL). IHC signals were generated with EnVision$^+$System-HRP (Dako North America, Inc) and substrate diaminobenzidine (Dako North America, Inc). Tissue sections were counterstained with Mayer Hematoxylin (Sigma-Aldrich, Inc), dehydrated with increasing concentrations (70%, 80%, 90%, and 100%) (vol/vol) of ethyl alcohol, incubated in 100% xylene for 20 minutes at room temperature, and mounted in Canada balsam (Sigma-Aldrich, Inc). A human melanoma and a normal skin FFPE tissue section were used as a positive and a negative control, respectively, to determine the staining specificity of mAb D2.8.5-C4B8. Cytoplasmic membrane staining was considered positive for CSPG4. The staining intensity was graded by semiquantitative analysis by two investigators (K. Sakakura and Y. Wang)—negative (–), when no staining was detected; weak (+), when the staining was weak; moderate (++), when the staining was homogeneous; strong (+++), when the staining was strong and homogeneous (32). The staining was done once.

Flow Cytometry Analysis

The tumor cells isolated from the pleural effusions of patients were stained with antibodies specific to various cell surface markers to assess the percentage of various cell populations by flow cytometry and identify CSCs as described by Al-Hajj et al. (33). Cells (1×10^6) were resuspended in phosphate-buffered saline (PBS; pH 7.4) (Invitrogen) containing 1% BSA in 96-well U-bottomed plates (Corning, Inc, Corning, NY) and incubated with the CSPG4-specific mAbs 225.28, 763.74, TP41.2, and TP61.5 (1 μg/mL for all mAbs) at 4°C for 30 minutes. After washing twice in PBS, cells were resuspended in PBS containing 1% BSA and incubated with rabbit anti-mouse IgG-PE antibody at 4°C for 30 minutes. After washing three times in PBS, cells were stained with mouse anti-human CD24-FITC mAb (1:10 dilution), mouse anti-human CD44-allophycocyanin mAb (1:10 dilution), mouse anti-human CD45-peridinin chlorophyll protein mAb (1:10 dilution), and stained with 7-aminoactinomycin D (1:10 dilution; Beckman Coulter, Marseille, France) (to exclude dead cells) at 4°C for 30 minutes. We used CD45 as a lineage (Lin) marker for the hematopoietic stem cells (Lin^-) because the cells that stain positive or negative for CD45-specific mAb also stain positive or negative for the lineage cocktail (mouse anti-human CD2, 3, 10, 16, 18, 31, 45, 64, and 140b)-specific mAbs (1:10 dilution was used for each mAb). In our study, the stem cell population was defined as $CD45^-Lin^-CD44^{hi}/CD24^{lo/-}$ cells based on the finding of Al-Hajj et al. After washing twice in PBS, cells were resuspended in PBS containing 1% BSA for flow cytometry analysis. Forty-five thousand gated events were analyzed by flow cytometry on a BD FACSCalibur using CellQuest software (Becton Dickinson and Company, San Jose, CA). The same staining procedure was used for breast cancer cell lines HS578T, MDA-MB-231, MDA-MB-435 and SUM149, MCF7, SK-BR-3, and T47D, excluding staining with the CD45-specific mAb.

Reverse Transcription–Polymerase Chain Reaction

Semiquantitative reverse transcription–polymerase chain reaction (RT-PCR) was performed as described earlier (34). The following primers were used to amplify and detect the CSPG4 gene, 5′-TGGCCTTCACTGTCACTGTCC-3′ (forward primer) and 5′-CACTTGCTTCTGGGCCGTCACTCG-3′ (reverse primer), designed by DNAstar (DNASTAR, Inc, Madison, WI). Total RNA was isolated from 1×10^6 MDA-MB-435 cells using Trizol Reagent (Invitrogen) according to the manufacturer's instructions. Purified RNA was treated with DNAseI (New England Biolabs, Beverly, MA) according to the manufacturer's instructions. cDNA synthesis was performed using Oligo-dT and M-MLV Reverse Transcriptase (Invitrogen). All RT-PCR assays were performed in 0.2 mL PCR Tube Strips (Fisher Scientific Company L.L.C., Kalamazoo, MI) using 0.5 μg cDNA and Taq DNA Polymerase (Invitrogen) in a final volume of 50 μL under the following conditions: 95°C for 5 minutes, 35 cycles of 30 seconds at 95°C, followed by 1 minute at 58°C and 1 minute at 72°C in a Gene Amp PCR System 9700 (Applied Biosystems, Foster City, CA). The RNA of each sample was normalized to the ACTB (actin, beta) mRNA level. The resulting PCR products were electrophoresed on 1.5% agarose gels, stained with ethidium bromide, and imaged with AlphaImagerTM2200 Documentation and Analysis System (Imgen Technologies, Alexandria, VA).

Immunoblot

The M14, M14/CSPG4, and MDA-MB-435 cells were cultured in RPMI 1640 medium with 10% fetal calf serum at 37°C.

MDA-MB-231 or MDA-MB-435 cells were seeded at the concentration of 2.0×10^4 per well in a 96-well plate in RPMI 1640 medium without serum and incubated at 37°C for 48 or 24 hours, respectively. Cells were then incubated with the CSPG4-specific mAb 225.28 (0.1 mg/mL), the control mAb F3-C25 (0.1 mg/mL), or PBS at 37°C for an additional 48 hours. Cells were lysed in lysis buffer (10 mM Tris–HCl [pH 8.2], 1% NP40, 1 mM EDTA, 0.1% BSA, 150 mM NaCl) containing 1/50 (vol/vol) of protease inhibitor cocktail (Calbiochem, La Jolla, CA). Cell lysates were also prepared from snap-frozen xenograft tumors that were homogenized and lysed in *glass homogenizers* (Kontes Glass Co, Vineland, NJ) in ice-cold radioimmunoprecipitation assay buffer (Thermo Scientific, Rockford, IL) containing 1/50 (vol/vol) of protease inhibitor cocktail (Calbiochem). After vortexing for 60 seconds, lysates were chilled on ice for 45 minutes and then centrifuged at 16 000*g* at 4°C for 30 minutes. Protein concentrations in the lysates were measured using the Bradford reagent (Bio-Rad Laboratories, Hercules, CA). Equal amounts of proteins (60 μg per well) from the clarified lysates were separated by sodium dodecyl sulfate–polyacrylamide gel electrophoresis and transferred to polyvinylidene fluoride membrane of 0.45-μm pore size (Millipore, Bedford, MA). After blocking the membranes with 5% nonfat dry milk plus 2% BSA at room temperature for 2 hours, membranes were incubated overnight at 4°C with CSPG4-specific mAb 763.74 (10 μg/mL), control mAb MK2-23 (10 μg/mL), mouse anti-phosphorylated human FAK (Tyr397) mAb (1:250 dilution), mouse anti-human FAK mAb (1:500 dilution), rabbit anti-phosphorylated human AKT (Ser473) mAb (1:1000 dilution), rabbit anti-human AKT mAb (1:1000 dilution), mouse anti-human ERK1/2 mAb (1:1000 dilution), rabbit anti-phosphorylated human ERK1/2 (Thr202/Tyr204) mAb (1:1000 dilution), mouse anti-human PKCα mAb (1:125 dilution), mouse anti-human calnexin mAb TO-5 (1 μg/mL), and mouse anti-HLA class I heavy chain mAb HC-10 (0.2 μg/mL). Then, peroxidase-conjugated secondary antibodies (anti-mouse IgG antibody, 1:5000 dilution; or anti-rabbit IgG antibody, 1:10 000 dilution) were added, and incubation was continued at room temperature for an additional 45 minutes. Between the incubations, membranes were washed five times, 5 minutes each, with PBS (pH 7.4) containing 0.1% Tween. Then, bound antibodies were detected using ECL Plus Western Blotting Detection System (GE Healthcare, Buckinghamshire, UK), and bands were visualized using the FOTO/Analyst Investigator Eclipse System (Fotodyne Incorporate, Hartland, WI). Band densities were quantified using the TotalLab TL100 software (Nonlinear Dynamics, Durham, NC). The HLA class I heavy chain and calnexin, detected with mAb HC-10 and mAb TO-5, respectively, were used as the protein loading controls.

Cell Growth, Adhesion, and Transmigration Assays In Vitro

To measure cell growth in vitro, MDA-MB-231 cells were grown in serum-free RPMI 1640 medium at 37°C for 48 hours. Cells were then seeded (5.0×10^4 cells per well) in a 96-well plate (Becton Dickinson and Company, Franklin Lakes, NJ) filled with Matrigel (BD Biosciences) and incubated with the CSPG4-specific mAb 225.28 (0.125 or 0.25 mg/mL), the control mAb F3-C25 (0.125 or 0.25 mg/mL), or PBS, in 200 μL serum-free RPMI 1640 medium per well, at 37°C in a 5% CO_2 atmosphere. At the end of day 2, 4, and 6, images of cultured cells were taken using a Zeiss Inverted Fluorescence Microscope (AxioVision Software; Carl Zeiss MicroImaging GmbH, Jena, DE). Cells were then harvested using Cell Recovery Solution (BD Biosciences), stained with trypan blue (Sigma-Aldrich, Inc) and counted using a hemocytometer (Hausser Scientific, Horsham, PA); cells stained with trypan blue were excluded (35,36). The results were expressed as percent inhibition of growth using the number of living cells incubated with PBS as a 100% reference. Incubation with mAb (0.25 mg/mL) for 6 days was selected for all cell growth experiments because the experimental conditions were optimal to detect differences in growth between mAb 225.28- and control mAb F3-C25-treated cells.

To measure cell adhesion, MDA-MB-435 cells were grown in serum-free RPMI 1640 medium at 37°C for 24 hours, seeded (2.0×10^5 cells per well) in a 96-well plate coated with fibronectin (12 μg/mL PBS), and incubated with the CSPG4-specific mAb 225.28 (0.05 mg/mL), the control mAb F3-C25 (0.05 mg/mL), or PBS, in 100 μL RPMI 1640 medium per well, at 37°C for 40 minutes in a 5% CO_2 atmosphere. At the end of the incubation, cells were washed in PBS to remove any nonadherent cells, and the adherent cells were fixed with 70% ethanol (vol/vol), stained with crystal violet (Sigma-Aldrich, Inc), and resuspended in PBS. The extent of cell adhesion was semiquantified by reading the optical density at 540 nm using a microplate reader (MTX Lab System, Inc, Vienna, VA). The results were expressed as percent inhibition of adhesion using the adhesion values of cells incubated with PBS as a 100% reference.

To measure cell migration, MDA-MB-231 cells were grown in serum-free RPMI 1640 medium at 37°C for 48 hours. Cells were then seeded (5.0×10^4 per well) in the top chamber of a 24-Transwell plate (8-μm pore size; BD Biosciences) and incubated with the CSPG4-specific mAb 225.28 (0.25 mg/mL), the control mAb F3-C25 (0.25 mg/mL), or PBS, in 100 μL serum-free RPMI 1640 medium per well, at 37°C in a 5% CO_2 atmosphere. All bottom chambers of the Transwell plate were filled with serum-free RPMI 1640 medium (600 μL per well) containing fibronectin (10 μg/mL; Sigma-Aldrich, Inc). At the end of day 2, migrated cells were stained with HEMA 3 stain set (Fisher Scientific Company L.L.C.) according to the manufacturer's instructions. The nonmigrated cells on the top side of the filter were removed by scrubbing twice with cotton tipped swab. The migrated cells on the bottom side of six randomly selected fields per well were then imaged and counted using a Zeiss Inverted Fluorescence Microscope (AxioVision Software, Carl Zeiss MicroImaging GmbH). The results were expressed as percent inhibition of migration using the number of migrated cells incubated with PBS as a 100% reference. All experiments were performed three independent times in triplicates.

In Vivo Studies

Early Experimental Lung Metastasis Model. Adult female severe combined immunodeficient (C.B17-SCID) mice (Taconic Farms, Inc, Hudson, NY), 8 weeks old and weighing 17–18 g, were injected into the tail vein with MDA-MB-231 cells (1.0×10^6 per mouse; n = 15 mice) or MDA-MB-435 cells (2.0×10^6 per mouse; n = 10 mice) resuspended in 200 μL PBS using 1-mL insulin syringe (Kendall Healthcare, Mansfield, MA) and $30_{1/2}$-gauge needle (BD Biosciences). On day 3, the mice injected with

MDA-MB-231 cells were randomly divided into two groups—one group of mice (n = 8) was injected into the tail vein with the CSPG4-specific mAb 225.28 (100 μg per injection) and the other group of mice (n = 7) was injected with the control mAb F3-C25 (100 μg per injection). The mice injected with MDA-MB-435 cells were randomly divided into two groups—one group of mice (n = 5) was injected into the tail vein with the mAb 225.28 (100 μg per injection) and the other group of mice (n = 5) was injected with the mAb F3-C25 (100 μg per injection). The injections were given twice weekly until the mice were killed by CO_2 asphyxiation. The mice injected with MDA-MB-231 cells were killed on day 79 (week 11) and those injected with MDA-MB-435 cells were killed on day 34 (week 5), also by CO_2 asphyxiation. Lungs were collected, fixed in Bouin fixative (Polysciences, Inc, Warrington, PA), the lobes were separated, and white pulmonary nodules, a common manifestation of lung metastasis, were counted using a dissecting microscope (magnification ×10) (Carl Zeiss Stemi DV4 Stereomicroscope, Carl Zeiss MicroImaging GmbH). The technician and the research fellow who injected the mAbs were blinded to the specificity of the mAbs. The research fellow who analyzed the lungs was blinded to the type of treatment received by the mice.

Late Experimental Lung Metastasis Model. Adult female SCID mice, 8 weeks old and weighing 17–18 g, were injected into the tail vein with MDA-MB-231 cells (1.0×10^6 per mouse; n = 16 mice) resuspended in 200 μL PBS. On day 20, two randomly selected mice were killed by CO_2 asphyxiation and the lungs were harvested and subjected to histological examination for the presence of metastatic nodules. Nodules were detected in both mice. At this time, the remaining 14 mice were randomized into two groups—one group of mice (n = 7) was injected into the tail vein with the CSPG4-specific mAb 225.28 (100 μg per injection) and the other group of mice (n = 7) was injected with the control mAb F3-C25 (100 μg per injection) every 48 hours, for a total of 3 injections. All mice were killed a day after the third injection, and the lungs were collected for analysis of the area of metastases as well as proliferation and apoptosis of tumor cells. The technician and the fellow who injected the mAbs were blinded to the specificity of the mAbs.

Analysis of Area of Established Lung Metastasis. For histological analysis of the area of lung metastasis, 4-μm thick FFPE sections of mouse lungs from SCID mice injected with MDA-MB-231 cells were stained with Mayer Hematoxylin (Sigma-Aldrich, Inc) and Eosin Y (0.5% alcoholic) solution (Sigma-Aldrich, Inc) according to the manufacturer's instructions. The areas of metastatic nodules in randomly selected five high-power fields per section (magnification ×200) were measured and calculated by the SPOT Advanced Imaging software (Diagnostic Instruments, Inc, Sterling Heights, MI). The values shown are the mean tumor area of each group. The research fellow who analyzed the lungs was blinded to the type of treatment received by the mice.

Analysis of Apoptosis in Established Lung Metastasis Model. To quantify the number of apoptotic cells in pulmonary nodules of lungs from mice injected with MDA-MB-231 cells, a Terminal deoxynucleotidyl transferase dUTP Nick End Labeling (TUNEL) assay was performed on 4-μm thick FFPE sections of mouse lungs using the ApopTag Plus Peroxidase In Situ Apoptosis Kit (S7101) (Millipore, Billerica, MA) according to the manufacturer's instructions. Apoptotic tumor cells were detected in lung tissue sections by the TUNEL assay and quantified by counting the number of apoptotic cells in 10 randomly selected fields per slide (magnification ×200). The values shown are the mean number of apoptotic tumor cells in each group. The number of apoptotic tumor cells was counted by a technician who was blinded to the type of treatment received by the mice.

Analysis of Mitotic Cells in Established Lung Metastasis Model. To identify the mitotic cells in pulmonary nodules of lungs from mice injected with MDA-MB-231 cells, 4-μm thick FFPE sections of mouse lungs were stained with rabbit anti-phosphorylated human Histone H3 (Ser10) antibodies (1:100 dilution) according to the manufacturer's instructions. Mitotic tumor cells in lung tissue sections were detected by staining phosphorylated Histone H3 (Ser10) protein and quantified by counting 10 random fields per section (magnification ×200). The values shown are the mean number of mitotic tumor cells in each group. The number of mitotic tumor cells was counted by a technician who was blinded to the type of treatment received by the mice.

IHC Staining of CD31 Protein in Postsurgery Orthotopic Breast Cancer Model

MDA-MB-435 cell–derived primary xenograft tumors were fixed with IHC Zinc Fixative (BD Biosciences) at room temperature for 24 hours and then embedded in paraffin blocks. Four-micrometer thick FFPE sections were stained with rat anti-mouse CD31 mAb (10 μg/mL) as described previously (37).

Tumor Recurrence and Metastasis in Postsurgery Orthotopic Breast Cancer Model

The MDA-MB-435 cells (2.0×10^6 per mouse), resuspended in 50 μL PBS, were injected into the mammary fat pad of female SCID mice (total n = 24; 6 weeks old; weighing 15–16 g) using 0.5-mL insulin syringe (Kendall Healthcare). On day 7, when tumors were palpable, mice were divided into two groups using a stratified randomization strategy, such that the mean tumor volume was not statistically significantly different between two groups ($P > .05$). Starting on day 7, one group of mice (n = 12) was injected intraperitoneally with the CSPG4-specific mAb 225.28 (100 μg per injection), twice weekly, for a total of 18 injections; the other group of mice (n = 12) was injected similarly with the control mAb F3-C25 (100 μg per injection). On day 79, orthotopic primary tumors were removed using the approved survival surgery protocol. After the surgery, mice were treated with the analgesic drug ketoprofen (Fort Dodge Animal Health, Fort Dodge, IA) diluted in PBS (5 mg/kg, subcutaneously injected) daily for 3 days. Treatment with antibodies was continued using the same regimen for nine additional injections. Local tumor recurrence was monitored twice weekly. On day 131, all mice were killed by CO_2 asphyxiation and the lungs were collected and examined for the number of surface metastatic nodules as described above. The technician and the fellow who injected the mAbs were blinded to the specificity of the mAbs. The metastatic nodules in the lungs removed from the mice were counted by a technician who was blinded to the type of treatment received by the mice.

Statistical Analysis

Statistical analyses for all quantitative studies, except the analysis of CSPG4 mRNA expression, were performed using a two-sample Student *t* test. The 95% confidence intervals (CIs) of means were calculated for the difference between two sample means as described by Armitage and Berry (38). All statistical analysis was performed using Microsoft Office Excel 2003 software. All two-sided *P* values less than or equal to .05 were considered significant.

Results

Expression of CSPG4 in Patient-Derived Breast Tumors, Breast Cancer Cell Lines, and CSCs From Pleural Effusions

Analysis of CSPG4 Expression in Primary Breast Tumors. To determine if CSPG4 was preferentially expressed in TNBC, we analyzed the CSPG4 mRNA levels in the following four subgroups of breast cancer cells, $ER^-/HER2^-$, $ER^-/HER2^+$, $ER^+/HER2^-$, and $ER^+/HER2^+$, using a publicly available, clinically annotated, breast cancer dataset (GSE5460). The status of PR expression was not available in this dataset. The CSPG4 gene expression level differed statistically significantly among the four subgroups ($P = .0238$; Kruskal–Wallis test) and was substantially higher in the $ER^-/HER2^-$ subgroup than in the other subgroups (nominal $P = .01$ to $.06$; Mann–Whitney U test); the $ER^-/HER2^-$ vs $ER^+/HER2^-$ comparison surpassed a Bonferroni threshold of .0167 (Figure 1, A).

The preferential expression of CSPG4 by $ER^-/HER2^-$ breast cancer cells determined by gene expression analysis was corroborated by IHC staining of breast cancer subtypes with the CSPG4-specific mAb. Expression of CSPG4 protein was noted in 32 of the 44 (72.7%) primary TNBC lesions. In contrast, CSPG4 protein was detected in only eight of the 28 (28.6%) ER^+ and three of the 18 (16.7%) $HER2^+$ breast cancer primary lesions, respectively (Table 1 and Figure 1, B).

Analysis of CSPG4 Expression on the Surface of Breast Cancer Cell Lines. Next, we investigated if CSPG4 protein was preferentially expressed on the surface of the TNBC cell lines. Flow cytometry analysis of four TNBC cell lines (HS578T, MDA-MB-231, MDA-MB-435, and SUM149) and three luminal breast cancer cell lines (MCF7, SK-BR-3, and T47D) using CSPG4-specific mAb 225.28 showed that CSPG4 expression was substantially higher on the surface of TNBC cell lines (Figure 1, C). Cells with a $CD44^{hi}/CD24^{lo/-}$ phenotype (CSC) were present at a frequency of approximately 92.5%–99.0% in the four TNBC cell lines. In contrast, cells with this phenotype were not detected in the SK-BR-3 cell line and were present at a frequency of 34.6% and 1.5% in the luminal breast cancer cell lines, MCF7 and T47D, respectively. Therefore, the frequency of CSCs was much higher in the TNBC cell lines than in the luminal breast cancer cell lines. A high percentage of CSC, approximately 66.7%–96.1%, showed high expression of CSPG4 (mean fluorescence intensity > 50) in the TNBC cell lines tested. In contrast, only a small percentage of CSC, approximately 1.5%–13.0%, showed a low or barely detectable expression of CSPG4 protein (mean fluorescence intensity = 4.6–12.0) in the three luminal breast cancer cell lines (Figure 1, C). Therefore, the CSC subpopulation of TNBC cells showed a differential expression of CSPG4 compared with luminal breast cancer cells.

A flow cytometry analysis showed that the distinct epitopes recognized by the CSPG4-specific mAbs 225.28, 763.74, TP41.2, and TP61.5 were differentially expressed by each cell line, in terms of percentage of stained cells and mean fluorescence intensity (Supplementary Table 1, top panel, available online). In the MDA-MB-435 cell line, at least 90% of the CSCs, expressed CSPG4 epitopes recognized by all four mAbs. In contrast, in the SUM149 cell line, approximately 96%, 3%, and 51% of the CSCs expressed CSPG4 epitopes recognized by the mAbs 225.28, 763.74, and TP61.5, respectively (Supplementary Table 1, bottom panel, available online). The expression patterns of CSPG4 epitopes on total cell populations were comparable to those on CSCs in the MDA-MB-435 and SUM149 cell lines. In contrast, expression of the CSPG4 epitopes recognized by mAb 763.74 and TP41.2 was lower on the surface of CSCs than on total cell populations in the HS578T and MDA-MB-231 cell lines (Supplementary Table 1, available online).

Analysis of CSPG4 Expression on the Surface of $CD44^{hi}/CD24^{lo/-}$ Cells From Pleural Effusions. Flow cytometry analysis of breast cancer cells isolated from pleural effusions of 14 breast cancer patients showed a varying subpopulation (0.71%–92.7%) of CSCs, defined as the $CD45^-Lin^-/CD44^{hi}/CD24^{lo/-}$ phenotype (Supplementary Table 2, available online). The percentage of cells with the $CD44^{hi}/CD24^{lo/-}$ phenotype within the $CD45^-Lin^-$ pleural effusion cell population was low (<10%) in nine patients, intermediate (18.6%–35.0%) in four patients, and high (92.7%) in one patient. Consistent with the CSC phenotype, the percentage of $CD44^{hi}/CD24^{lo/-}$ cells in total cell population of pleural effusions ranged from 0.01% to 0.89% (Supplementary Table 2, available online). Twelve of the 14 patients were available to analyze the CSC cell population for CSPG4 expression with the four CSPG4-specific mAbs (Table 2). CSPG4-positive ($CSPG4^+$) cells in the $CD45^-$ population contained a markedly increased (1.5- to 19.5-fold) percentage of CSC compared with the total $CD45^-$ cell population. The percentage of the CSC-enriched subpopulation in a $CSPG4^+$ population differed (mean = 7.14-fold, 95% CI = 4.09 to 10.19) depending on the CSPG4-specific mAb used (Table 2). Representative results from the pleural effusions of four patients that showed different enrichment patterns of CSC cell population with the CSPG4-specific mAbs 225.28 and 763.74 are shown in Figure 1, D. This observation was consistent with the heterogeneous expression observed for CSPG4 epitopes defined by different mAbs in different cell lines (Supplementary Table 1, available online).

Analysis of the Molecular Characteristics of CSPG4 Expressed by Breast Cancer Cells

To define the molecular basis of the reactivity of CSPG4-specific mAb with the TNBC cell lines, we assessed the CSPG4 mRNA level in the MDA-MB-435 cell line by semiquantitative RT-PCR (Supplementary Figure 1, A, available online) because this cell line showed the highest level of CSPG4 expression

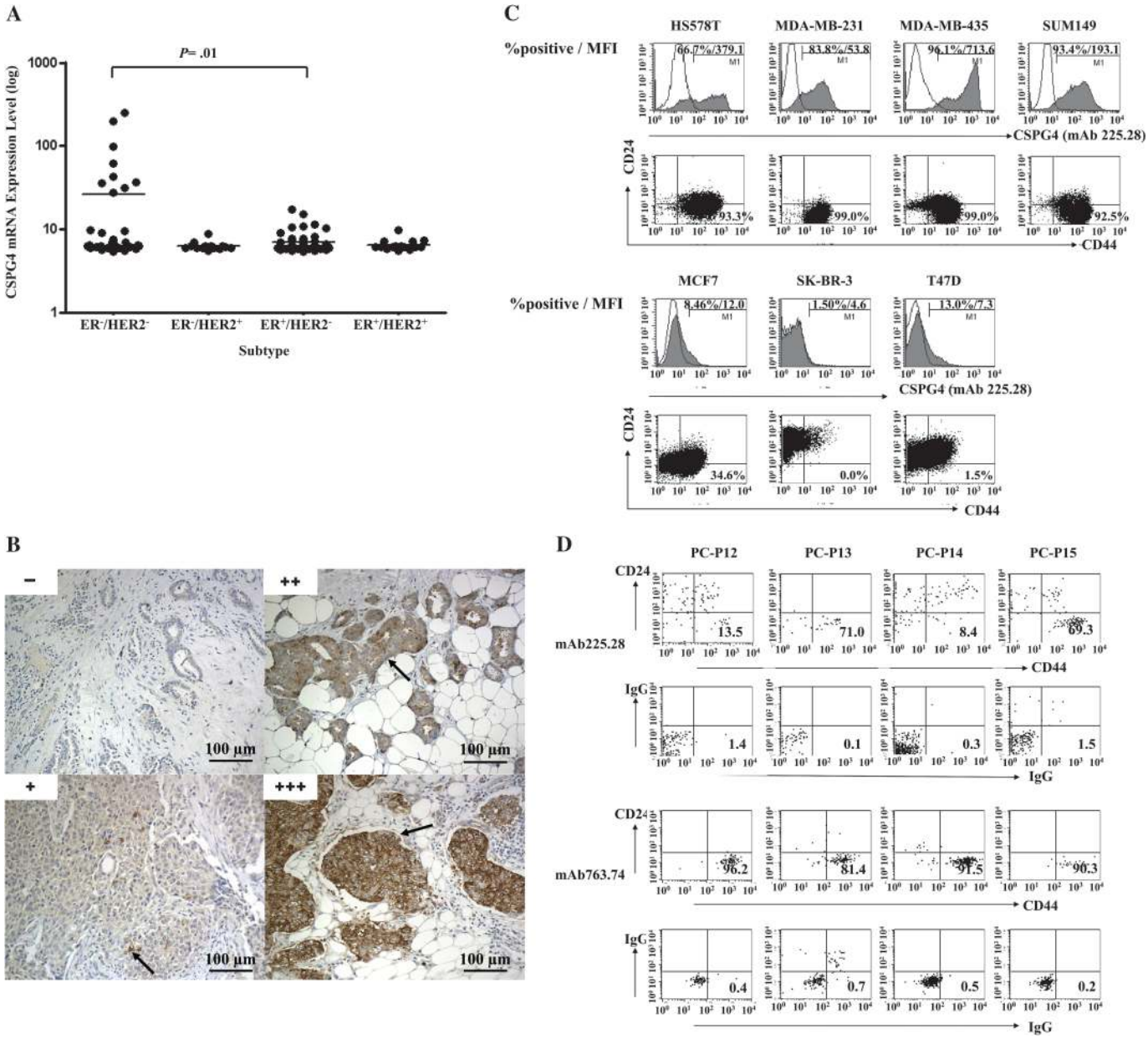

Figure 1. Analysis of chondroitin sulfate proteoglycan 4 (CSPG4) expression in breast cancer subtypes. **A**) Analysis of CSPG4 mRNA expression levels in published clinical microarray datasets (GSE5460). **Closed circles** represent individual patients, and **horizontal bars** denote the mean expression. CSPG4 mRNA expression level is statistically significantly higher in estrogen receptor–negative (ER^-)/$HER2^-$ breast cancers than in $ER^-/HER2^+$, $ER^+/HER2^-$, and $ER^+/HER2^+$ breast cancers. The *P* value determined by the Mann–Whitney *U* test ($ER^-/HER2^-$ vs $ER^+/HER2^-$, $P = .01$) surpassed a Bonferroni threshold of .0167. **B**) Analysis of CSPG4 protein expression in triple-negative breast cancer (TNBC) lesions. Representative images of immunohistochemical (IHC) staining of TNBC lesions (**arrow marked**) stained with the CSPG4-specific monoclonal antibody (mAb) D2.8.5-C4B8 are shown. The staining was graded as – (negative), when no staining was detected; + (weak), when the staining was weak; ++ (moderate), when the staining was homogeneous; +++ (strong), when the staining was strong and homogeneous. The IHC staining was performed once. Magnification ×200. Scale bar = 100 µm. **C**) Analysis of CSPG4 protein expression and frequency of $CD44^{hi}/CD24^{lo/-}$ cells in TNBC cell lines HS578T, MDA-MB-231, MDA-MB-435, and SUM149 and in luminal cell lines MCF7, SK-BR-3, and T47D. Cells were treated either with CSPG4-specific mAb 225.28 and rabbit anti-mouse IgG-PE antibodies or with mouse anti-human CD24-FITC mAb, mouse anti-human CD44-allophycocyanin mAb, and 7-aminoactinomycin D. Stained cells were subjected to flow cytometry analysis. The percentage of cells stained with the CSPG4-specific mAb 225.28 and the mean fluorescence intensity (MFI) are shown in each histogram (% positive/MFI). **D**) Enrichment of CSC subpopulation in $CSPG4^+$ cell population in pleural effusions from patients with breast carcinoma. After exclusion of dead cells, $CD45^-/CSPG4^+$ cells stained with CSPG4-specific mAb 225.28 (**top panel**) or mAb 763.74 (**bottom panel**) were analyzed for CD44 and CD24 expression. The percentages of $CD44^{hi}/CD24^{lo/-}$ cells found in four patient samples (PC-P12, PC-P13, PC-P14, and PC-P15) are indicated in the bottom right quadrant of the dot plots.

(Supplementary Table 1, top panel, available online). Immunoblot analysis with CSPG4-specific mAb 763.74 detected two components with the molecular weight of 280 kDa and greater than 440 kDa; these two components were previously reported in melanoma cell lysates (15) (Supplementary Figure 1, B, available online).

Table 1. Differential expression of chondroitin sulfate proteoglycan 4 (CSPG4) protein in breast cancer subtypes*

CSPG4 expression (grade)†	No. of ER+ tumors/total (%)	No. of HER2+ tumors/total (%)	No. of ER−/PR−/HER2− tumors/total (%)
Negative (−)	20/28 (71.4)	15/18 (83.3)	12/44 (27.3)
Weak (+)	6/28 (21.4)	3/18 (16.7)	10/44 (22.7)
Moderate (++)	2/28 (7.2)	0/18 (0.0)	18/44 (40.9)
Strong (+++)	0/28 (0.0)	0/18 (0.0)	4/44 (9.1)

* Breast cancer subtypes were based on ER, PR, and HER2 expression in primary tumors. Immunohistochemistry (IHC) staining was performed using CSPG4-specific monoclonal antibody (mAb) D2.8.5-C4B8. The ER−/PR−/HER2− tumors were the triple-negative breast cancer subtype. ER = estrogen receptor; PR = progesterone receptor.

† Semiquantitative analysis of IHC staining of the cytoplasmic membrane with the CSPG4-specific mAb D2.8.5-C4B8. The staining was graded as − (negative), when no staining was detected; + (weak), when the staining was weak; ++ (moderate), when the staining was homogeneous; +++ (strong), when the staining was strong and homogeneous. The IHC staining was performed once.

Effect of CSPG4-Specific mAb 225.28 on Growth, Adhesion, and Migration of TNBC Cell Lines In Vitro

Induction of CSPG4 expression on the surface of human melanoma cells showed enhanced growth, adhesion, and/or migration of the cells in vitro, and similar results were obtained with nerve/glial antigen 2, the rat homolog of CSPG4, when expressed on the surface of rat glioma or mouse melanoma cells (39–41). Therefore, next, we investigated if the CSPG4-specific mAb 225.28, which could bind to all the TNBC cell lines tested (Figure 1, C), was able to block TNBC cell growth, adhesion, and migration in vitro. MDA-MB-231 and MDA-MB-435 cell lines were selected for this study because approximately 84% and 96% of the cells, respectively, express CSPG4 protein. The density and morphology of the cells at the end of the incubation in a three-dimensional Matrigel culture is shown in Figure 2, A. The viable cells not stained by trypan blue were indicative of cell growth; these cells were counted and the results showed that in three-dimensional cell cultures, mAb 225.28 inhibited the growth of MDA-MB-231 cells by approximately 70% (mAb 225.28 vs control mAb, mean = 74.4% vs 1.4%; difference of mean = 73.0%, 95% CI = 55.5% to 90.5%; $P < .001$) (Figure 2, B). Furthermore, mAb 225.28 inhibited MDA-MB-435 cell adhesion to fibronectin by 44.8% (mAb 225.28 vs control mAb, mean = 44.8% vs −1.8%; difference of mean = 46.7%, 95% CI = 34.8% to 58.5%; $P < .001$) (Figure 2, C), and MDA-MB-231 cell migration toward fibronectin by 56.8% (mAb 225.28 vs control mAb, mean = 56.8% vs 0.4%; difference of mean = 56.4%, 95% CI = 47.2% to 65.6%; $P < .001$) (Figure 2, D). Therefore, these results showed that CSPG4 protein played a role in growth, adhesion, and migration of the TNBC cells.

Effect of CSPG4-Specific mAb 225.28 on Signaling Pathways Important for Cell Growth, Adhesion, and Migration In Vitro

To investigate the molecular mechanisms underlying the in vitro antitumor activity of CSPG4-specific mAb 225.28, we analyzed the effect on signaling pathways that are activated by CSPG4 and are involved in growth, adhesion, and migration of tumor cells. They include the FAK and ERK1/2 pathways that play an important role in cytoskeleton reorganization, as well as growth, adhesion, and migration of cells (41,42). In addition, CSPG4 is involved in PKCα-mediated enhanced cell migration and phosphatidylinositol 3-kinase/AKT-mediated increased survival and chemoresistance

Table 2. Enrichment of cancer stem cell subpopulation in CSPG4+ cells in pleural effusions from patients with breast cancer*

Patient sample	$CD44^{hi}/CD24^{lo/-}$ population in $CD45^{-}Lin^{-}$ cells (%)	Percent of $CD44^{hi}/CD24^{lo/-}$ cells in $CSPG4^{-}$ cells (fold enrichment)					
		CSPG4-specific mAb 225.28	CSPG4-specific mAb 763.74	CSPG4-specific mAb TP41.2	CSPG4-specific mAb TP61.5	Average value of the four CSPG4-specific mAbs†	Highest value of the four CSPG4-specific mAbs
PC-P4	2.91	8.6 (2.96)	5.7 (1.96)	10.2 (3.51)	24.7 (8.49)	12.3 (4.23)	24.7 (8.49)
PC-P5	16.3	26.8 (1.64)	68.9 (4.23)	23.7 (1.45)	18.3 (1.12)	34.4 (2.11)	68.9 (4.23)
PC-P6	7.21	4.7 (0.65)	0.0 (0.00)	3.57 (0.50)	50.0 (6.93)	14.6 (2.02)	50.0 (6.93)
PC-P7	19.2	35.5 (1.85)	95.4 (4.97)	61.3 (3.19)	75.4 (3.93)	66.9 (3.48)	95.4 (4.97)
PC-P8	18.0	2.9 (0.16)	60.7 (3.37)	20.9 (1.16)	31.3 (1.74)	29.0 (1.61)	60.7 (3.37)
PC-P9	3.38	22.6 (6.69)	40.2 (11.90)	38.5 (11.40)	35.7 (10.60)	34.3 (10.10)	40.2 (11.90)
PC-P10	31.6	91.5 (2.90)	96.8 (3.06)	93.7 (2.97)	94.8 (3.00)	94.2 (2.98)	96.8 (3.06)
PC-P11	13.0	67.4 (5.18)	93.3 (7.18)	70.3 (5.41)	75.5 (5.81)	76.6 (5.89)	93.3 (7.18)
PC-P12	4.94	13.5 (2.73)	96.2 (19.50)	90.3 (18.3)	67.3 (13.60)	66.8 (13.5)	96.2 (19.50)
PC-P13	11.6	71.0 (6.12)	81.4 (7.02)	68.7 (5.92)	76.7 (6.61)	74.5 (6.42)	81.4 (7.02)
PC-P14	12.2	8.4 (0.69)	91.5 (7.50)	49.1 (4.02)	32.0 (2.62)	45.3 (3.71)	91.5 (7.50)
PC-P15	58.7	69.3 (1.18)	90.3 (1.54)	ND	ND	79.8 (1.36)	90.3 (1.54)
Average‡	16.59	35.2 (2.73)	68.4 (6.02)	48.2 (5.25)	52.9 (5.86)	52.4 (4.78)	74.1 (7.14)

* Tumor cells were isolated from the pleural effusions of 12 patients with metastatic breast cancer and incubated sequentially with the chondroitin sulfate proteoglycan 4 (CSPG4)–specific monoclonal antibodies (mAbs) (225.28, 763.74, TP41.2, or TP61.5), phycoerythrin-labeled anti-mouse IgG antibodies, and fluorescein isothiocyanate–labeled anti-CD24, allophycocyanin-labeled anti-CD44, peridinin chlorophyll protein–labeled anti-CD45 antibodies, and 7-aminoactinomycin D (7-AAD). Stained cells were subjected to flow cytometry analysis. The percentages of $CD44^{hi}/CD24^{lo/-}$ cells in the $CD45^{-}$/7-AAD^{-} population and in the $CD45^{-}$/7-AAD^{-}/$CSPG4^{+}$ population were determined. Enrichment of $CD44^{hi}/CD24^{lo/-}$ population by gating at $CSPG4^{+}$ cells was calculated by dividing the percentage of $CD44^{hi}/CD24^{lo/-}$ cells in the $CD45^{-}$/7-AAD^{-}/$CSPG4^{+}$ population by that in the $CD45^{-}$/7-AAD^{-} population; fold enrichment is shown in parenthesis. ND = Not done.

† The average % (fold enrichment) of $CD44^{hi}/CD24^{lo/-}$ in $CSPG4^{+}$ cells, detected by four different CSPG4-specific mAbs, in each patient sample.

‡ The average % (fold enrichment) of $CD44^{hi}/CD24^{lo/-}$ in $CSPG4^{+}$ cells, detected by four different CSPG4-specific mAbs, in all 12 patient samples.

of tumor cells (43,44). These pathways are all activated in TNBC and associated with TNBC progression (45,46). In vitro incubation with the CSPG4-specific mAb 225.28 showed a decrease in the level of phosphorylated FAK (Tyr397), phosphorylated AKT (Ser473), and phosphorylated ERK1/2 (Thr202/Tyr204) in the MDA-MB-231 and MDA-MB-435 cell lines. In addition, the total protein levels of FAK, ERK1/2, AKT, and PKCα were also decreased (Figure 3). These results indicated that the in vitro antitumor activity of mAb 225.28 may be mediated by inhibition of several signaling pathways involved in growth, adhesion, and migration of tumor cells.

Effect of CSPG4-Specific mAb 225.28 on Early Experimental Metastasis of TNBC Cells

Next, we assessed the in vivo antitumor activity of CSPG4-specific mAb 225.28 in an experimental lung metastasis model, induced by injecting MDA-MB-231 cells into SCID mice. This cell line was chosen because it has a high percentage (99%) of CSC, and a medium to high level of CSPG4 expression (mean fluorescence intensity = 53.8) (Figure 1, C). On day 79, the number of pulmonary nodules was less by greater than 96.8% in the mice treated with the CSPG4-specific mAb 225.28 compared with the mice treated with the control mAb F3-C25 (mAb 225.28 vs control mAb, mean = 11.5 vs 362.3 nodules on lung surface; difference of mean = 350.8 nodules, 95% CI = 236.1 to 465.5 nodules; $P = .008$) (Figure 4, A).

Similar results were obtained in an experimental lung metastasis model induced by injecting MDA-MB-435 cells into SCID mice. These cells also express the CSC phenotype in 99% of the cells but have a much higher level of CSPG4 expression (mean fluorescence intensity = 713.6) compared with the MDA-MB-231 cells (Figure 1, C). On day 34, the number of pulmonary nodules was less by greater than 81.1% by the CSPG4-specific mAb 225.28 compared with the control mAb F3-C25 (mAb 225.28 vs control mAb, mean = 146.8 vs 776.4 nodules on lung surface; difference of mean = 629.6 nodules, 95% CI = 250.6 to 1008.6 nodules; $P = .003$) (Figure 4, B).

Effect of CSPG4-Specific mAb 225.28 on Late Experimental Metastasis of TNBC Cells

We further examined if CSPG4-specific mAb 225.28 was able to cause regression of established experimental lung metastasis

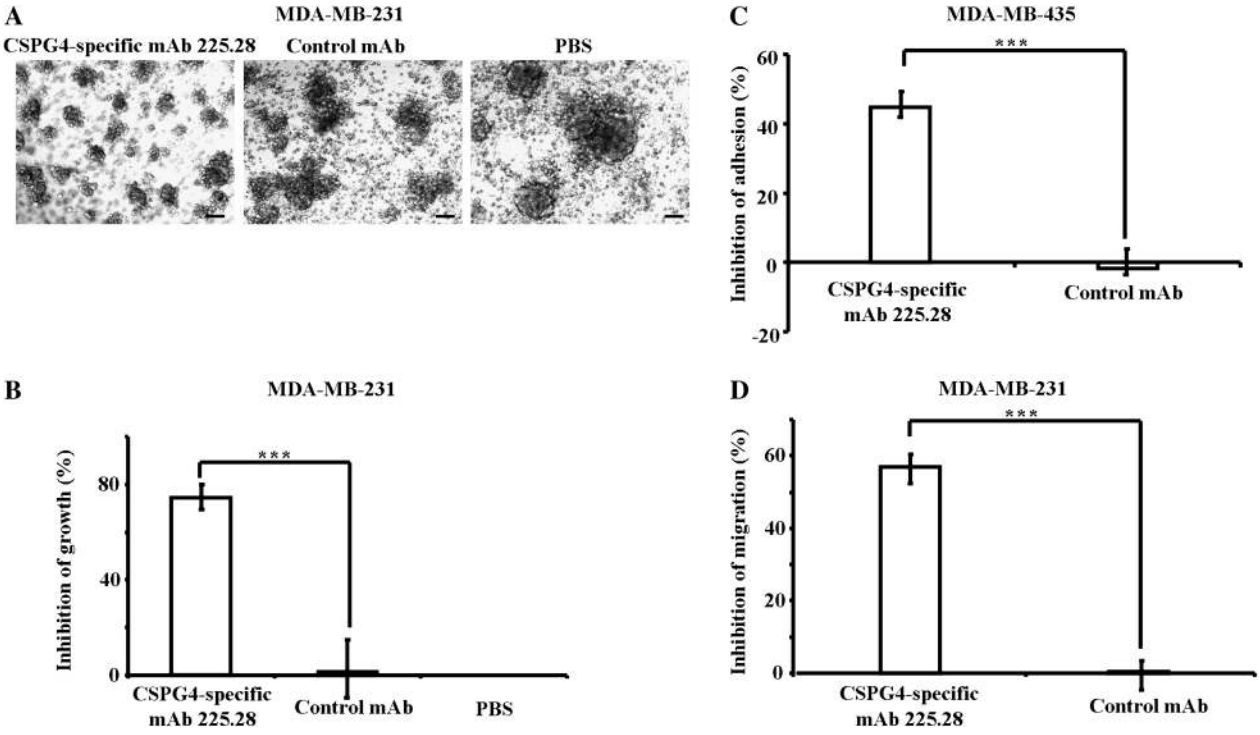

Figure 2. Effect of chondroitin sulfate proteoglycan 4 (CSPG4)–specific monoclonal antibody (mAb) 225.28 on triple-negative breast cancer (TNBC) cell growth, adhesion, and transmigration in vitro. **A)** Image analysis of TNBC cell growth in the presence of mAb 225.28. MDA-MB-231 cells were incubated with mAb 225.28, the control mAb F3-C25, or phosphate-buffered saline (PBS), at 37°C for 6 days in a 96-well filled with Matrigel. Representative images show the clusters of cells. Magnification ×100. Scale bar =100 μm. **B)** Quantitative analysis of TNBC cell growth. The viable cells that were not stained by trypan blue were counted. The results are expressed as percent inhibition of cell growth using the values obtained in the PBS-treated cells as a 100% reference. The means and 95% confidence intervals from three independent experiments are shown. ***$P < .001$. **C**) Quantitative analysis of TNBC cell adhesion to fibronectin. MDA-MB-435 cells were incubated at 37°C for 40 minutes with mAb 225.28, mAb F3-C25, or PBS in an adhesion assay. Adherent cells were quantitated by measuring the optical density at 540 nm. The results are expressed as percent inhibition of adhesion using the values obtained from PBS-treated cells as a 100% reference. The means and 95% confidence intervals from three independent experiments are shown. ***$P < .001$. **D**) Quantitative analysis of TNBC cell migration. MDA-MB-231 cells were incubated for 48 hours at 37°C with mAb 225.28, mAb F3-C25, or PBS in a transmigration assay. Cells that migrated toward fibronectin were counted. The results are expressed as percent inhibition of migration using the values obtained from PBS-treated cells as a 100% reference. The means and 95% confidence intervals from three independent experiments are shown. ***$P < .001$. All P values were calculated using the two-sided Student t test.

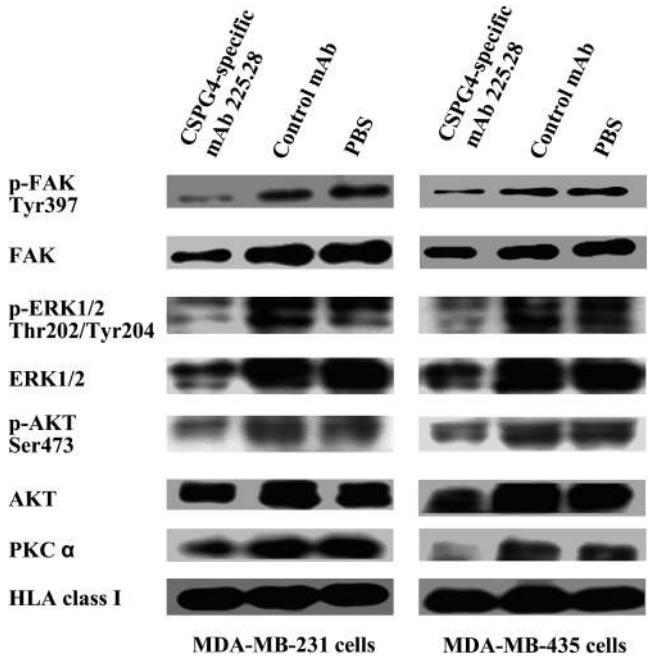

Figure 3. Effect of chondroitin sulfate proteoglycan 4 (CSPG4)–specific monoclonal antibody (mAb) 225.28 on signaling pathways important for cell growth, adhesion, and migration in vitro. MDA-MB-231 and MDA-MB-435 cells were treated with CSPG4-specific mAb 225.28, the control mAb F3-C25, or phosphate-buffered saline (PBS) at 37°C for 48 hours. Representative immunoblot analysis of p-FAK (Tyr397), FAK, p-ERK1/2 (Thr202/Tyr204), ERK1/2, p-AKT (Ser473), AKT, and PKCα is shown. HLA class I heavy chain was used as the loading control. The experiment was performed three independent times. p = phosphorylated.

induced with MDA-MB-231 cells in SCID mice. On day 25, the area of lung metastasis was quantified in lungs removed from mice treated with mAb 225.28 or the control mAb F3-C25. The area of 20-day-old metastatic nodules was smaller by approximately 73.1% in mice treated with mAb 225.28 compared with the nodules in mice treated with the control mAb F3-C25 (mAb 225.28 vs control mAb, mean = 44590.8 vs 165950.8 μm^2; difference of mean = 121360.0 μm^2, 95% CI = 91010.7 to 151709.4 μm^2; $P < .001$) (Figure 4, D). We then investigated if there was a higher number of apoptotic cells in the metastatic pulmonary nodules of mice treated with the CSPG4-specific mAb 225.28. Lungs from mice treated with the control mAb F3-C25 were used as controls (Figure 4, E). The number of apoptotic cells was approximately 69.8% higher in pulmonary nodules from mice treated with mAb 225.28, compared with mice treated with the control mAb F3-C25 (mAb 225.28 vs control mAb, mean = 59.9 vs 18.1 apoptotic cells; difference of mean = 41.8 apoptotic cells, 95% CI = 15.2 to 68.2 apoptotic cells; $P = .01$) (Figure 4, F). Furthermore, the number of mitotic cells in the same pulmonary nodules was quantified by analyzing the expression of phosphorylated Histone H3 protein (47) (Figure 4, G). The number of mitotic cells was lower by approximately 68.8% in the metastatic lesions from mice treated with mAb 225.28 compared with mice treated with the control mAb F3-C25 (mAb 225.28 vs control mAb, mean = 3.0 vs 9.6 mitotic cells; difference of mean = 6.6 mitotic cells, 95% CI = 3.2 to 9.9 mitotic cells; $P = .002$) (Figure 4, H).

Effect of CSPG4-Specific mAb 225.28 on Tumor Recurrence, Metastasis, and Density of Blood Vessels in a Postsurgery Orthotopic Breast Cancer Model

Effect of CSPG4-Specific mAb 225.28 on Spontaneous Metastasis and Tumor Recurrence After Surgical Resection of Primary Tumors. To assess the potential clinical significance of the antitumor activity of CSPG4-specific mAb 225.28, we tested its ability to inhibit spontaneous metastasis and recurrence of orthotopic mammary tumors after surgical removal of the primary tumors on day 79. The mice (n = 12) treated with the CSPG4-specific mAb 225.28 showed statistically significant reduced levels of spontaneous lung metastases after surgery compared with mice (n = 12) treated with the control mAb F3-C25. All 12 mice in the control group developed metastases, whereas there was no metastasis in two mice and statistically significantly reduced metastasis in the remaining 10 mice (mAb 225.28 vs control mAb, mean = 14.55 vs 161.73 pulmonary nodules; difference of mean = 147.17 pulmonary nodules, 95% CI = 15.39 to 278.95 pulmonary nodules; $P = .04$) (Figure 5, A).

The mice treated with the CSPG4-specific mAb 225.28 also showed statistically significantly reduced tumor recurrence after surgical removal of the primary tumors; recurrences were detected in only two of the 12 mice treated with mAb 225.28 as compared with eight of the 12 mice treated with the control mAb F3-C25 (mAb 225.28 vs control, mean = 16.7% vs 66.7%; difference of mean = 50.0%, 95% CI = 14.0% to 86.0%; $P = .01$) (Figure 5, B). These results indicated that CSPG4-specific mAb 225.28 inhibited both tumor metastasis and tumor recurrence after surgical removal of orthotopic mammary primary tumors.

Effect of CSPG4-Specific mAb 225.28 on Density of Blood Vessels in Primary Xenograft Tumors. The expression of CSPG4 protein is increased in activated pericytes in a tumor microenvironment, similar to its mouse homolog, and the CSPG4-specific mAb 225.28 also cross-reacts with mouse CSPG4 (data not shown). Therefore, we compared the vascular density in mammary fat pad primary xenograft tumors removed from mice treated with mAb 225.28 and the control mAb F3-C25 (Figure 5, C) using CD31-specific mAb as a probe to detect vascular density. Tumors from mice treated with mAb 225.28 showed a statistically significantly decrease in vascular density compared with tumors from mice treated with mAb F3-C25 (mAb 225.28 vs control, mean = 47.0 vs 69.7 blood vessels; difference of mean = 22.7 blood vessels, 95% CI = 5.6 to 39.8 blood vessels; $P = .02$) (Figure 5, D).

Effect of CSPG4-Specific mAb 225.28 on Signaling Pathways Important for Cell Growth, Adhesion, and Migration in Primary Xenograft Tumors

To investigate whether CSPG4-specific mAb 225.28 also inhibits the signaling pathways in vivo, we analyzed xenograft tumors from mice treated with mAb 225.28 or control mAb for changes in the levels of total and phosphorylated FAK, ERK1/2, and AKT proteins, and total PKCα protein (Figure 6, A). A densitometric analysis showed that the levels of phosphorylated proteins of the three key signaling pathways associated with CSPG4 function were statistically significantly reduced in the mammary fat pad primary xenograft tumors treated with the CSPG4-specific mAb

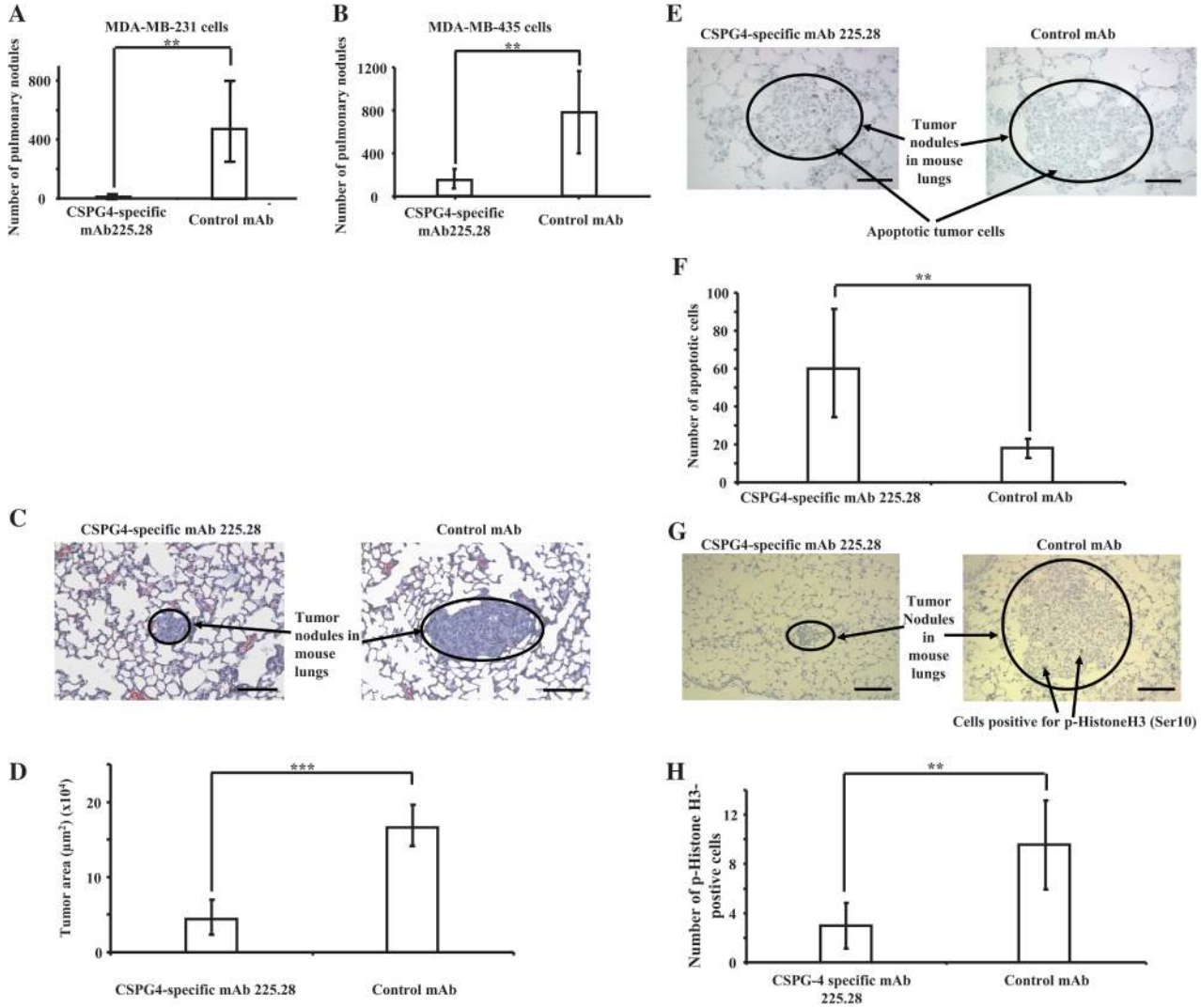

Figure 4. Effect of chondroitin sulfate proteoglycan 4 (CSPG4)–specific monoclonal antibody (mAb) 225.28 on the metastasis of triple-negative breast cancer cells in an experimental lung metastasis model. **A**) Analysis of MDA-MB-231 cell metastasis. Mice were injected intravenously with MDA-MB-231 cells (1×10^6 cells in 200 μL phosphate-buffered saline [PBS] per mouse) and were randomized into two groups on day 3. One group (n = 8) was injected intravenously twice weekly with mAb 225.28, and the other group (n = 7) was injected with the control mAb F3-C25. Lungs were analyzed for metastatic nodules on day 79. Means and 95% confidence intervals from two independent experiments are shown. $^{**}P < .01$. **B**) Analysis of MDA-MB-435 cell metastasis. On day 3, mice were injected intravenously with MDA-MB-435 cells (1×10^6 in 200 μL PBS per mouse) and randomized into two groups. One group of mice (n = 5) was injected intravenously twice weekly with mAb 225.28, and the other group of mice (n = 5) was injected with the control mAb F3-C25. Lungs were analyzed for metastatic nodules on day 34. Means and 95% confidence intervals from two independent experiments are shown. $^{**}P < .01$. **C**) Analysis of the effect of CSPG4-specific mAb 225.28 on established experimental lung metastases. Mice were injected intravenously with MDA-MB-231 cells (1×10^6 in 200 μL PBS per mouse) and randomized into two groups. On day 20, one group of mice (n = 7) was injected intravenously with mAb 225.28 every 48 hours, three times, and the other group of mice (n = 7) was injected with mAb F3-C25 using the same schedule and dose as mAb 225.28. Lungs were collected on day 25 and formalin-fixed paraffin-embedded lung tissues were stained with hematoxylin and eosin. Representative images are shown. Magnification ×200. Scale bar = 100 μm. **D**) Quantitative analysis of tumor areas shown in (**C**). The area of metastatic nodules in each section was quantified from five randomly selected high-power (magnification ×200) fields. Means and 95% confidence intervals from two independent experiments are shown. $^{***}P < .001$. **E**) Analysis of apoptotic tumor cells in lung metastasis from mice treated with the CSPG4-specific mAb 225.28. Representative images are shown. Magnification ×200. Scale bar =100 μm. **F**) Quantitative analysis of the apoptotic cells shown in (**E**) from 10 randomly selected high-power (magnification ×200) fields per section. Means and 95% confidence intervals from two independent experiments are shown. $^{**}P < .01$. **G**) Analysis of mitotic cells in metastatic tumors in lung tissue sections from mice treated with the CSPG4-specific mAb 225.28. Mitotic cells were detected by staining p-Histone H3 (Ser10) protein. Representative images are shown. Magnification ×200. Scale bar = 100 μm. **H)** Quantitative analysis of mitotic cells shown in (**G**) from 10 randomly selected high-power (magnification ×200) fields per section. Means and 95% confidence intervals from two independent experiments are shown. ** $P < .01$. All P values were calculated using the two-sided Student t test.

225.28 compared with tumors from mice treated with the control mAb F3-C25 (phosphorylated FAK [Tyr397] [mAb 225.28 vs control, mean = 0.8% vs 13.9%; difference of mean = 13.1%, 95% CI = 10.3% to 15.6%; $P < .001$], phosphorylated ERK1/2 [Thr202/Tyr204] [mAb 225.28 vs control, mean = 1.4% vs 5.3%; difference of mean = 3.9%, 95% CI = 2.8% to 4.9%; $P = .001$], and phosphorylated AKT [Ser473] [mAb 225.28 vs control, mean = 4.1% vs 16.3%; difference of mean = 12.3%, 95% CI = 9.4% to 15.2%;

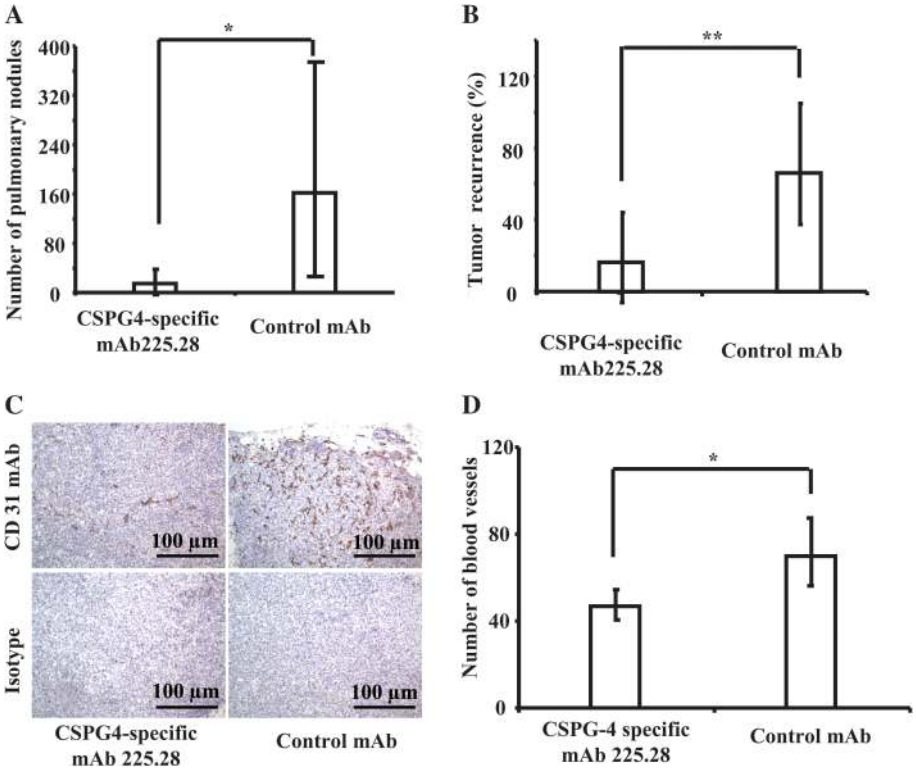

Figure 5. Effect of chondroitin sulfate proteoglycan 4 (CSPG4)–specific monoclonal antibody (mAb) 225.28 on spontaneous metastases of triple-negative breast cancer cells and tumor recurrence in the postsurgery recurrence and metastasis model. MDA-MB-435 cells (1.0×10^6 in 50 μL phosphate-buffered saline per mouse) were injected into the mammary fat pad of female severe combined immunodeficient mice (n = 24). On day 7, mice were randomized into two groups using a stratified randomization strategy. Starting on day 7, one group (n = 12) was injected intraperitoneally with mAb 225.28 twice weekly for a total of 18 injections, and the other group (n = 12) was injected with the control mAb F3-C25. On day 79, all tumors were surgically removed. The treatment with mAb was continued with nine additional injections. **A**) On day 131, lungs were collected for quantitative analysis of metastatic nodules. Means and 95% confidence intervals from three independent experiments are shown. $*P < .05$. **B**) Mice were monitored twice weekly for local tumor recurrence. Results are expressed as the percent of mice treated with mAb 225.28 and control mAb F3-C25 that developed local tumor recurrence. $**P = .01$. **C**) Analysis of the effect of CSPG4-specific mAb 225.28 on the density of blood vessels in surgically removed primary tumors. Blood vessels in MDA-MB-435 cell–derived primary tumors were detected by staining with CD31-specific mAb. Representative images are shown. Magnification ×400. Scale bar = 100 μm. **D**) Quantitative analysis of the blood vessels shown in (**C**) by counting five randomly selected high-power (magnification ×400) fields per section. Means and 95% confidence intervals from three independent experiments are shown. $*P < .05$. All *P* values were calculated using the two-sided Student *t* test.

$P < .001$]). The total amount of PKCα protein was also statistically significantly reduced in the primary tumors from mice treated with the CSPG4-specific mAb 225.28 compared with mice treated with the control mAb F3-C25 (mAb 225.28 vs control, mean = 1.1% vs 11.8%; difference = 10.7%, 95% CI = 3.4% to 18.1%; $P = .012$) (Figure 6, B).

Discussion

This study has shown for the first time that the membrane-bound CSPG4 is differentially expressed in breast cancer subtypes with a significantly higher frequency in basal-like breast cancer and TNBC subtypes, compared with luminal subtypes, both in breast cancer cell lines and in patient-derived lesions. Additionally, CSPG4 protein was also expressed on the surface of tumor cells isolated from pleural effusions of breast cancer patients, and there was an association between the level of CSPG4 protein expression and the frequency of CSCs in the pleural effusions; this association was also noted in TNBC cell lines. More importantly, targeting TNBC cells with the CSPG4-specific mAb 225.28 inhibited their growth and migration in vitro and showed inhibition of tumor growth and metastasis in human TNBC tumor xenografts in immunodeficient mice. The CSPG4-specific mAb 225.28 also inhibited the regrowth of orthotopic primary tumors that were removed and limited the progression of metastatic lesions in surgically treated mice. The effects were associated with the reduction of proliferation and induction of apoptosis of tumor cells in metastatic lesions; reduction of vascular density in the tumor microenvironment; and inhibition of activation of key signaling pathways regulating cell proliferation, migration, and survival, both in vitro and in vivo. These results clearly indicate the potential usefulness of therapeutically targeting the CSPG4 protein in breast tumors with a TNBC phenotype.

In this study, the higher expression of CSPG4 in TNBC, compared with luminal breast cancer, was observed both in the CSC (cells with $CD44^{hi}/CD24^{lo/-}$ phenotype) subpopulation as well as the differentiated tumor cells. This observation was not unique to CSPG4 because a similar expression pattern was described for other molecules including epidermal growth factor receptor, cytokeratins 5 and 6, S-phase kinase-associated protein 2, and mesenchyme forkhead 1 (also known as forkhead box C2 [FOXC2]) (31,48,49). Whether the differential CSPG4 expression in TNBC and other breast cancer subtypes reflects the different cell types from which they originate, or differences in the regulation of gene expression in different subtypes of breast cancer, remains to be determined. In contradistinction, the absence or low level of CSPG4 expression in subtypes of breast cancer other than TNBC is not likely to reflect loss of the encoding gene because loss of genetic material from chromosome 15 where CSGP4 has been mapped (50) has not been documented in those subtypes of breast cancer. Although the molecular mechanisms underlying the preferential expression of CSPG4 protein in TNBC were not fully elucidated in our study, the findings demonstrated the potential use of CSPG4 protein as a diagnostic biomarker and as a therapeutic target.

Because cells with CSC phenotype are known to have a high invasive potential, a highly enriched CSC subpopulation in the TNBC cell lines used in our experiments may have played a major

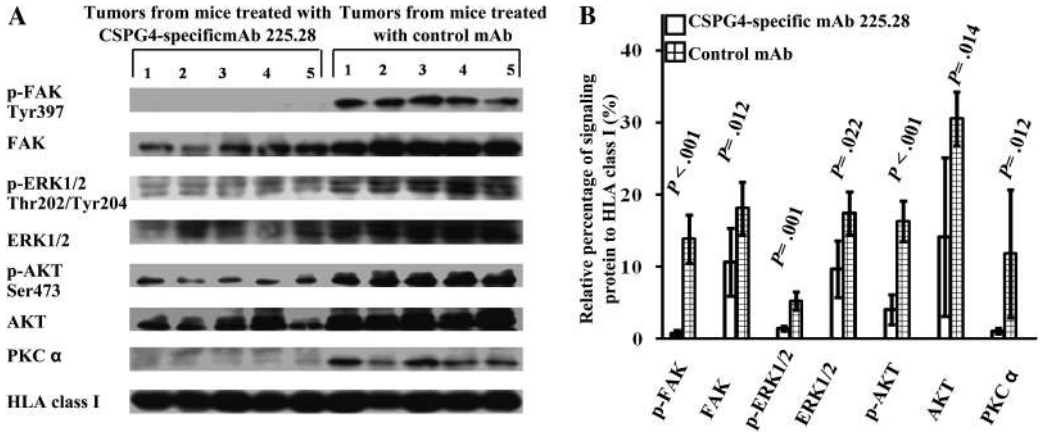

Figure 6. Effect of chondroitin sulfate proteoglycan 4 (CSPG4)–specific monoclonal antibody (mAb) 225.28 on signaling pathways important for cell growth, adhesion, and migration in vivo. MDA-MB-435 cells (1.0×10^6 in 50 μL phosphate-buffered saline per mouse) were injected into the mammary fat pad of female SCID mice. **A**) On day 79, orthotopic primary tumors that originated from MDA-MB-435 cells were surgically removed from mice (n = 5 per group) treated with mAb 225.28 and control mAb F3-C25. Cell lysates were analyzed by immunoblot assay, and representative immunoblot of two independent experiments shows the levels of p-FAK (Tyr397), FAK, p-ERK1/2 (Thr202/Tyr204), ERK1/2, p-AKT (Ser473), AKT, and PKCα. HLA class I heavy chain was used as the loading control. p = phosphorylated. **B**) Quantitative densitometric analysis of the proteins shows the ratios of the density of each protein to the reference HLA class I heavy chain. Means and 95% confidence intervals from two independent experiments are shown. All *P* values were calculated using the two-sided Student *t* test.

role in tumor progression and metastatic spread of cancer cells to lungs—a common site of metastasis associated with TNBC (7,51,52). The CSC phenotype is also expressed by the majority of cancer cells detected in the bone marrow of breast cancer patients (53). Given the important role of CSPG4 protein in migration, metastasis and chemoresistance of malignant cells (39,40,42,43,54–56), as well as its expression on pericytes (57), which may be the origin of mesenchymal cells (58), it is tempting to speculate that the core protein of this cell surface proteoglycan may contribute to the stem cell–like properties of the CSC subpopulation and to the epithelial–mesenchymal transition (59). The morphologic transdifferentiation enables the carcinoma cells to acquire a mesenchymal appearance and gene expression profile that contributes to increased migration and invasiveness during malignant progression (60–62).

The CSPG4-specific mAb 225.28 was effective in inhibiting metastasis of the TNBC cell lines, MDA-MB-231 and MDA-MB-435. Although, MDA-MB-231 is a well-established human breast cancer cell line, the nature of MDA-MB-435 as a breast cancer cell line is disputed (63). According to some investigators, the MDA-MB-435 cell line has properties consistent with a melanoma origin, whereas according to others, the MDA-MB-435 cell line, which was isolated from the pleural effusion of a patient with breast cancer, has a gene expression profile consistent with a breast cancer origin (64–67). Despite its historically controversial origin, the MDA-MB-435 cell line proved to be a useful tool in our study to establish the proof of principle that CSPG4-targeted therapy is effective for inhibiting the growth, metastasis, and tumor recurrence of aggressive metastatic cell populations that have a high percentage (99%) of cells expressing the $CD44^+CD24^{-/lo}$ phenotype as well as the CSPG4 protein.

The CSPG4-specific mAb 225.28 inhibited the activation of multiple signaling pathways important for the malignant progression of TNBC (45,46). The pleiotropic effect of CSPG4-specific mAb on TNBC cells resembles that of other currently used therapeutic mAb, such as trastuzumab, which targets both the phosphatidylinositol 3-kinase/AKT survival signaling pathway and the mitogen-activated protein kinase growth signaling pathway (68,69). However, unlike trastuzumab, the CSPG4-specific mAb 225.28 did not mediate cell-dependent cytotoxicity (70) of TNBC cells because in vivo depletion of natural killer cells had no impact on its therapeutic efficacy (data not shown). Furthermore, mAb 225.28 did not mediate complement-dependent cytotoxicity (70) of CSPG4-positive tumor cells (data not shown). Collectively, these data indicate that the antitumor activity of CSPG4-specific mAb 225.28 was a direct result of its ability to inhibit signaling pathways important for the malignant progression of breast tumor cells.

There are significant efforts to target certain proteins, such as the sonic hedgehog and wingless-type MMTV integration site family, member 1–related signaling pathways that are associated with a "stem cell–like" tumor phenotype (71). However, targeting these molecules has the potential disadvantage to cause side effects because of their role in normal stem cell maintenance and function (72,73). In contrast, targeting CSPG4 with mAb is not expected to cause negative effects such as potential toxicity because the viability and fertility of CSPG4 null mice (74,75) argue against a critical role of this molecule for the maintenance and self-renewal of normal stem cells. In support of this possibility are two lines of evidence—first, side effects have not been documented in humans who have developed CSPG4-specific immunity either spontaneously or following immunizations (18,76); and second, general toxicity, such as body weight loss and delay in wound healing, has not been observed in mice treated with two systemic administrations per week of CSPG4-specific mAb 225.28 for 6 months (data not shown). The exquisite specificity of CSPG4-specific mAb may render them ideally suited for targeting highly tumorigenic and metastatic cell subpopulations within malignant tumors, and the current results argue in favor of developing clinical trials for therapeutic evaluation in TNBC patients.

From a methodological point of view, it is noteworthy that we tested the therapeutic efficacy of the CSPG4-specific mAb-based

immunotherapy in a postsurgical tumor recurrence and metastasis model instead of the widely used primary xenotransplant model because the former model, despite being technically challenging and time consuming, is closer to the actual clinical setting. In this setting, the main cause of death is not from primary tumors, which can be resected, but from local recurrence and distant metastasis of tumors.

This study has a few limitations. First, only a small number of patient-derived breast cancer tumors were tested for CSPG4 expression. Second, patient-derived TNBC lesions have not been used to assess the antitumor activity of CSPG4-specific mAb 225.28 in mice. To address these limitations, in some ongoing studies we are evaluating CSPG4 expression in a large number of different subtypes of breast cancer lesions to associate CSPG4 expression with the histopathological characteristics of the lesions and clinical course of the disease. Furthermore, we are evaluating the antitumor activity of mAb 225.28 in xenograft tumors established in mice from patient-derived TNBC lesions.

Supplementary Data

Supplementary data can be found at http://www.jnci.oxfordjournals.org/.

References

1. van 't Veer LJ, Dai H, van de Vijver MJ, et al. Gene expression profiling predicts clinical outcome of breast cancer. *Nature.* 2002;415:530–536.
2. Sorlie T, Tibshirani R, Parker J, et al. Repeated observation of breast tumor subtypes in independent gene expression data sets. *Proc Natl Acad Sci U S A.* 2003;100:8418–8423.
3. Sotiriou C, Neo SY, McShane LM, et al. Breast cancer classification and prognosis based on gene expression profiles from a population-based study. *Proc Natl Acad Sci U S A.* 2003;100:10393–10398.
4. Perou CM, Sorlie T, Eisen MB, et al. Molecular portraits of human breast tumours. *Nature.* 2000;406:747–752.
5. Rakha EA, El-Sayed ME, Green AR, et al. Biologic and clinical characteristics of breast cancer with single hormone receptor positive phenotype. *J Clin Oncol.* 2007;25:4772–4778.
6. Rakha EA, Tan DS, Foulkes WD, et al. Are triple-negative tumours and basal-like breast cancer synonymous? *Breast Cancer Res.* 2007;9:404. author reply 5.
7. Gluz O, Liedtke C, Gottschalk N, Pusztai L, Nitz U, Harbeck N. Triple-negative breast cancer—current status and future directions. *Ann Oncol.* 2009;20:1913–1927.
8. Eyler CE, Rich JN. Survival of the fittest: cancer stem cells in therapeutic resistance and angiogenesis. *J Clin Oncol.* 2008;26:2839–2845.
9. O'Brien CA, Kreso A, Jamieson CH. Cancer stem cells and self-renewal. *Clin Cancer Res.* 2010;16:3113–3120.
10. Honeth G, Bendahl PO, Ringner M, et al. The CD44+/CD24- phenotype is enriched in basal-like breast tumors. *Breast Cancer Res.* 2008;10:R53.
11. Nakshatri H, Srour EF, Badve S. Breast cancer stem cells and intrinsic subtypes: controversies rage on. *Curr Stem Cell Res Ther.* 2009;4:50–60.
12. Park SY, Lee HE, Li H, Shipitsin M, Gelman R, Polyak K. Heterogeneity for stem cell-related markers according to tumor subtype and histologic stage in breast cancer. *Clin Cancer Res.* 2010;16:876–887.
13. Giatromanolaki A, Sivridis E, Fiska A, Koukourakis MI. The CD44+/CD24- phenotype relates to 'triple-negative' state and unfavorable prognosis in breast cancer patients. *Med Oncol.* 2010. doi:10.1007/s12032-010-9530-3.
14. Petrelli F, Cabiddu M, Ghilardi M, Barni S. Current data of targeted therapies for the treatment of triple-negative advanced breast cancer: empiricism or evidence-based? *Expert Opin Investig Drugs.* 2009;18:1467–1477.
15. Campoli MR, Chang CC, Kageshita T, Wang X, McCarthy JB, Ferrone S. Human high molecular weight-melanoma-associated antigen (HMW-MAA): a melanoma cell surface chondroitin sulfate proteoglycan (MSCP) with biological and clinical significance. *Crit Rev Immunol.* 2004;24:267–296.
16. Wilson BS, Imai K, Natali PG, Ferrone S. Distribution and molecular characterization of a cell-surface and a cytoplasmic antigen detectable in human melanoma cells with monoclonal antibodies. *Int J Cancer.* 1981;28:293–300.
17. Wang X, Wang Y, Yu L, et al. CSPG4 in cancer: multiple roles. *Curr Mol Med.* 2010;10:419–429.
18. Mittelman A, Chen ZJ, Yang H, Wong GY, Ferrone S. Human high molecular weight melanoma-associated antigen (HMW-MAA) mimicry by mouse anti-idiotypic monoclonal antibody MK2-23: induction of humoral anti-HMW-MAA immunity and prolongation of survival in patients with stage IV melanoma. *Proc Natl Acad Sci U S A.* 1992;89:466–470.
19. Neve RM, Chin K, Fridlyand J, et al. A collection of breast cancer cell lines for the study of functionally distinct cancer subtypes. *Cancer Cell.* 2006;10:515–527.
20. Sabe I, Andritsch I, Mangoud A, Awad AS, Khalifa A, Krishan A. Flow cytometric analysis of estrogen receptor expression in isolated nuclei and cells from mammary cancer tissues. *Cytometry.* 1999;36:131–139.
21. Gritzapis AD, Baxevanis CN, Missitzis I, et al. Quantitative fluorescence cytometric measurement of estrogen and progesterone receptors: correlation with the hormone binding assay. *Breast Cancer Res Treat.* 2003;80:1–13.
22. Luo W, Hsu JC, Tsao CY, Ko E, Wang X, Ferrone S. Differential immunogenicity of two peptides isolated by high molecular weight-melanoma-associated antigen-specific monoclonal antibodies with different affinities. *J Immunol.* 2005;174:7104–7110.
23. Perosa F, Ferrone S. Syngeneic antiidiotypic monoclonal antibodies to the murine anti-HLA-DR, DP monoclonal antibody CR11-462. *Hum Immunol.* 1988;23:255–269.
24. Kusama M, Kageshita T, Chen ZJ, Ferrone S. Characterization of syngeneic antiidiotypic monoclonal antibodies to murine anti-human high molecular weight melanoma-associated antigen monoclonal antibodies. *J Immunol.* 1989;143:3844–3852.
25. Chen ZJ, Yang H, Kageshita T, Ferrone S. Human high-molecular-weight melanoma-associated antigen mimicry by mouse antiidiotypic monoclonal antibody TK7-371. *Cancer Res.* 1991;51:4790–4797.
26. Temponi M, Gold AM, Ferrone S. Binding parameters and idiotypic profile of the whole immunoglobulin and Fab' fragments of murine monoclonal antibody to distinct determinants of the human high molecular weight-melanoma associated antigen. *Cancer Res.* 1992;52:2497–2503.
27. Ogino T, Wang X, Kato S, Miyokawa N, Harabuchi Y, Ferrone S. Endoplasmic reticulum chaperone-specific monoclonal antibodies for flow cytometry and immunohistochemical staining. *Tissue Antigens.* 2003;62:385–393.
28. Stam NJ, Spits H, Ploegh HL. Monoclonal antibodies raised against denatured HLA-B locus heavy chains permit biochemical characterization of certain HLA-C locus products. *J Immunol.* 1986;137:2299–2306.
29. Temponi M, Kageshita T, Perosa F, Ono R, Okada H, Ferrone S. Purification of murine IgG monoclonal antibodies by precipitation with caprylic acid: comparison with other methods of purification. *Hybridoma.* 1989;8:85–95.
30. Lu X, Lu X, Wang ZC, Iglehart JD, Zhang X, Richardson AL. Predicting features of breast cancer with gene expression patterns. *Breast Cancer Res Treat.* 2008;108:191–201.
31. Cheang MC, Voduc D, Bajdik C, et al. Basal-like breast cancer defined by five biomarkers has superior prognostic value than triple-negative phenotype. *Clin Cancer Res.* 2008;14:1368–1376.
32. Kageshita T, Kuriya N, Ono T, et al. Association of high molecular weight melanoma-associated antigen expression in primary acral lentiginous melanoma lesions with poor prognosis. *Cancer Res.* 1993;53:2830–2833.
33. Al-Hajj M, Wicha MS, Benito-Hernandez A, Morrison SJ, Clarke MF. Prospective identification of tumorigenic breast cancer cells. *Proc Natl Acad Sci U S A.* 2003;100:3983–3988.
34. Luo W, Wang X, Kageshita T, Wakasugi S, Karpf AR, Ferrone S. Regulation of high molecular weight-melanoma associated antigen (HMW-MAA) gene expression by promoter DNA methylation in human melanoma cells. *Oncogene.* 2006;25:2873–2884.

35. Breitman TR, Selonick SE, Collins SJ. Induction of differentiation of the human promyelocytic leukemia cell line (HL-60) by retinoic acid. *Proc Natl Acad Sci U S A.* 1980;77:2936–2940.
36. Wu WJ, Tu S, Cerione RA. Activated Cdc42 sequesters c-Cbl and prevents EGF receptor degradation. *Cell.* 2003;114:715–725.
37. Ko E, Luo W, Peng L, Wang X, Ferrone S. Mouse dendritic-endothelial cell hybrids and 4-1BB costimulation elicit antitumor effects mediated by broad antiangiogenic immunity. *Cancer Res.* 2007;67:7875–7884.
38. Armitage P, Berry G. *Statistical Methods in Medical Research.* 3rd ed. London: Blackwell; 1994.
39. Burg MA, Nishiyama A, Stallcup WB. A central segment of the NG2 proteoglycan is critical for the ability of glioma cells to bind and migrate toward type VI collagen. *Exp Cell Res.* 1997;235:254–264.
40. Burg MA, Grako KA, Stallcup WB. Expression of the NG2 proteoglycan enhances the growth and metastatic properties of melanoma cells. *J Cell Physiol.* 1998;177:299–312.
41. Yang J, Price MA, Neudauer CL, et al. Melanoma chondroitin sulfate proteoglycan enhances FAK and ERK activation by distinct mechanisms. *J Cell Biol.* 2004;165:881–891.
42. Makagiansar IT, Williams S, Mustelin T, Stallcup WB. Differential phosphorylation of NG2 proteoglycan by ERK and PKCalpha helps balance cell proliferation and migration. *J Cell Biol.* 2007;178:155–165.
43. Makagiansar IT, Williams S, Dahlin-Huppe K, Fukushi J, Mustelin T, Stallcup WB. Phosphorylation of NG2 proteoglycan by protein kinase C-alpha regulates polarized membrane distribution and cell motility. *J Biol Chem.* 2004;279:55262–55270.
44. Chekenya M, Krakstad C, Svendsen A, et al. The progenitor cell marker NG2/MPG promotes chemoresistance by activation of integrin-dependent PI3K/Akt signaling. *Oncogene.* 2008;27:5182–5194.
45. Umemura S, Yoshida S, Ohta Y, Naito K, Osamura RY, Tokuda Y. Increased phosphorylation of Akt in triple-negative breast cancers. *Cancer Sci.* 2007;98:1889–1892.
46. Abeyweera TP, Chen X, Rotenberg SA. Phosphorylation of alpha6-tubulin by protein kinase Calpha activates motility of human breast cells. *J Biol Chem.* 2009;284:17648–17656.
47. Hendzel MJ, Wei Y, Mancini MA, et al. Mitosis-specific phosphorylation of histone H3 initiates primarily within pericentromeric heterochromatin during G2 and spreads in an ordered fashion coincident with mitotic chromosome condensation. *Chromosoma.* 1997;106:348–360.
48. Korsching E, Packeisen J, Agelopoulos K, et al. Cytogenetic alterations and cytokeratin expression patterns in breast cancer: integrating a new model of breast differentiation into cytogenetic pathways of breast carcinogenesis. *Lab Invest.* 2002;82:1525–1533.
49. Mani SA, Yang J, Brooks M, et al. Mesenchyme Forkhead 1 (FOXC2) plays a key role in metastasis and is associated with aggressive basal-like breast cancers. *Proc Natl Acad Sci U S A.* 2007;104:10069–10074.
50. Rettig WJ, Real FX, Spengler BA, Biedler JL, Old LJ. Human melanoma proteoglycan: expression in hybrids controlled by intrinsic and extrinsic signals. *Science.* 1986;231:1281–1284.
51. Matthay RA, Coppage L, Shaw C, Filderman AE. Malignancies metastatic to the pleura. *Invest Radiol.* 1990;25:601–619.
52. Fenton KN, Richardson JD. Diagnosis and management of malignant pleural effusions. *Am J Surg.* 1995;170:69–74.
53. Balic M, Lin H, Young L, et al. Most early disseminated cancer cells detected in bone marrow of breast cancer patients have a putative breast cancer stem cell phenotype. *Clin Cancer Res.* 2006;12:5615–5621.
54. Eisenmann KM, McCarthy JB, Simpson MA, et al. Melanoma chondroitin sulphate proteoglycan regulates cell spreading through Cdc42, Ack-1 and p130cas. *Nat Cell Biol.* 1999;1:507–513.
55. Fang X, Burg MA, Barritt D, Dahlin-Huppe K, Nishiyama A, Stallcup WB. Cytoskeletal reorganization induced by engagement of the NG2 proteoglycan leads to cell spreading and migration. *Mol Biol Cell.* 1999; 10:3373–3387.
56. Stallcup WB, Dahlin-Huppe K. Chondroitin sulfate and cytoplasmic domain-dependent membrane targeting of the NG2 proteoglycan promotes retraction fiber formation and cell polarization. *J Cell Sci.* 2001;114:2315–2325.
57. Schlingemann RO, Rietveld FJ, de Waal RM, Ferrone S, Ruiter DJ. Expression of the high molecular weight melanoma-associated antigen by pericytes during angiogenesis in tumors and in healing wounds. *Am J Pathol.* 1990;136:1393–1405.
58. Crisan M, Yap S, Casteilla L, et al. A perivascular origin for mesenchymal stem cells in multiple human organs. *Cell Stem Cell.* 2008;3:301–313.
59. Yang J, Price MA, Li GY, et al. Melanoma proteoglycan modifies gene expression to stimulate tumor cell motility, growth, and epithelial-to-mesenchymal transition. *Cancer Res.* 2009;69:7538–7547.
60. Hay ED. An overview of epithelio-mesenchymal transformation. *Acta Anat (Basel).* 1995;154:8–20.
61. Thiery JP. Epithelial-mesenchymal transitions in tumour progression. *Nat Rev Cancer.* 2002;2:442–454.
62. Fidler IJ. The pathogenesis of cancer metastasis: the 'seed and soil' hypothesis revisited. *Nat Rev Cancer.* 2003;3:453–458.
63. Rae JM, Ramus SJ, Waltham M, et al. Common origins of MDA-MB-435 cells from various sources with those shown to have melanoma properties. *Clin Exp Metastasis.* 2004;21:543–552.
64. Ross DT, Scherf U, Eisen MB, et al. Systematic variation in gene expression patterns in human cancer cell lines. *Nat Genet.* 2000;24:227–235.
65. Ellison G, Klinowska T, Westwood RF, Docter E, French T, Fox JC. Further evidence to support the melanocytic origin of MDA-MB-435. *Mol Pathol.* 2002;55:294–299.
66. Rae JM, Creighton CJ, Meck JM, Haddad BR, Johnson MD. MDA-MB-435 cells are derived from M14 melanoma cells—a loss for breast cancer, but a boon for melanoma research. *Breast Cancer Res Treat.* 2007;104:13–19.
67. Chambers AF. MDA-MB-435 and M14 cell lines: identical but not M14 melanoma? *Cancer Res.* 2009;69:5292–5293.
68. Sliwkowski MX, Lofgren JA, Lewis GD, Hotaling TE, Fendly BM, Fox JA. Nonclinical studies addressing the mechanism of action of trastuzumab (Herceptin). *Semin Oncol.* 1999;26:60–70.
69. Baselga J, Albanell J, Molina MA, Arribas J. Mechanism of action of trastuzumab and scientific update. *Semin Oncol.* 2001;28:4–11.
70. Herberman RB, Reynolds CW, Ortaldo JR. Mechanism of cytotoxicity by natural killer (NK) cells. *Annu Rev Immunol.* 1986;4:651–680.
71. Reya T, Morrison SJ, Clarke MF, Weissman IL. Stem cells, cancer, and cancer stem cells. *Nature.* 2001;414:105–111.
72. Palma V, Lim DA, Dahmane N, et al. Sonic hedgehog controls stem cell behavior in the postnatal and adult brain. *Development.* 2005;132:335–344.
73. Reya T, Clevers H. Wnt signalling in stem cells and cancer. *Nature.* 2005;434:843–850.
74. Kadoya K, Fukushi J, Matsumoto Y, Yamaguchi Y, Stallcup WB. NG2 proteoglycan expression in mouse skin: altered postnatal skin development in the NG2 null mouse. *J Histochem Cytochem.* 2008;56:295–303.
75. Huang FJ, You WK, Bonaldo P, Seyfried TN, Pasquale EB, Stallcup WB. Pericyte deficiencies lead to aberrant tumor vascularizaton in the brain of the NG2 null mouse. *Dev Biol.* 2010;344:1035–1046.
76. Erfurt C, Sun Z, Haendle I, et al. Tumor-reactive CD4+ T cell responses to the melanoma-associated chondroitin sulphate proteoglycan in melanoma patients and healthy individuals in the absence of autoimmunity. *J Immunol.* 2007;178:7703–7709.

Funding

This work was supported by the Empire Grant NYSDOH C017927 and the Elsa U. Pardee Foundation (X.W.), by the PHS grants P50-CA068438 (H.K.L.), R01 CA95447 (T.M.C.), R01 CA082295 (J.B.M.), R01 CA105500, R01 CA113861, and R01 CA138188 (S.F.), awarded by the National Cancer Institute and by the Kislak-Fields Family Fund (T.M.C.).

Notes

T. Osada and Y. Wang contributed equally to this work. T. M. Clay is the co-senior author.

The authors are solely responsible for the study design; collection, analysis, and interpretation of the data; decision to submit the article for publication; and writing of the article.

Present address: Department of Otolaryngology, Asahikawa Medical College, Asahikawa, Japan (A. Katayama).

The authors thank Lindsay L. Mock, Tissue Bank, Magee Women's Hospital of University of Pittsburgh Medical Center for providing human breast tissue sections, and Xiaojuan Deng and Tomoko Koya, technicians

at Ferrone's laboratory, for preparation of mAb and immunohistochemical staining of tissues. In addition, the authors thank Dr Joji Iida, Department of Cell Biology, Windber Research Institute, Windber, PA, and Dr Daniel P. Normolle and William E. Gooding, Department of Biostatistics, University of Pittsburgh Cancer Institute, for constructive criticisms and helpful discussions.

Affiliations of authors: University of Pittsburgh Cancer Institute, Pittsburgh, PA (XW, YW, LY, KS, AK, SF); Department of Immunology (XW, LY, SF), Department of Surgery (YW, KS, AK, SF), Department of Medicine (AB), and Department of Pathology (MC, SF), School of Medicine, University of Pittsburgh, Pittsburgh, PA; Department of Surgery (TO, HKL, TMC), Department of Medicine (DSH), Department of Biostatistics and Bioinformatics (WTB), Department of Immunology (HKL, TMC), and Department of Pathology (HKL), Duke University Comprehensive Cancer Center, Duke University Medical Center, Durham, NC; Department of Laboratory Medicine and Pathology and Masonic Cancer Center, University of Minnesota, Minneapolis, MN (JBM); Department of Pathology, Roswell Park Cancer Institute, Buffalo, NY (TK).